8-29-2019

Initial development of a prototype sensor testbed for fetal monitoring

Christian Beauvais
Rowan University

INITIAL DEVELOPMENT OF A PROTOTYPE SENSOR TESTBED FOR FETAL MONITORING

By

Christian Beauvais

A Thesis

Submitted to the
Department of Mechanical Engineering
College of Engineering
In partial fulfillment of the requirement
For the degree of
Master of Science in Mechanical Engineering
at
Rowan University
May 3, 2019

Thesis Chair: Wei Xue, Ph.D., and Francis Mac Haas, Ph.D.

Dedications

I would like to dedicate this manuscript to my family, my sisters Laurie Beauvais and Christelle Beauvais, my mother Kately Beauvais and grandmother Yvanne Dasme who always believe in me and pushed me to do my best. I also dedicate my thesis to my cousins, aunts and uncles and friends.

Acknowledgments

Primarily, I would like to thank God for my life and all other aspects of my life. Without his guidance, I would not be where I am. I would like to thank him for giving me the following characteristics such as strength, persistence, and hardworking. I would like to express my appreciation to my advisors Dr. Wei Xue and Dr. Francis Mac Haas for their guidance, encouragement and patience during my thesis. I would like to thank them for believing and not giving up on me. I would like to send special thanks to the other members of my committee. I would like to thank Professor Melanie Amadoro and Dr. Jennifer Kadlowec for agreeing to serve on my committee.

I would like to thank, God, my grandmother, mother, sister, aunts, and uncles, for sculpting me into the person that I am today. I would like to thank them for the encouragement and the support.

Special thanks to Muhammad Usman, Joseph Iannello, and Mehdi Benmassaoud, Harrison Hones, Taissa Michel for their advice, suggestions and help in this project. Finally, I would like to thank the Mechanical Engineering Department and The College of Engineering for providing the space and resources for conducting my project.

Abstract

Christian Beauvais
INITIAL DEVELOPMENT OF A PROTOTYPE SENSOR TESTBED FOR FETAL MONITORING
2018-2019
Wei Xue, Ph.D., and Francis Mac Haas, Ph.D.
Master of Science in Mechanical Engineering

The objective of this research is to design and manufacture a device that exhibits some of the bio-physiological signals relevant to fetal health monitoring. Currently, limited options exist for testing the performance of monitoring devices such as the tocodynamometer (TOCO) and electrocardiograph (ECG) that measure the bio-physiological signals of a woman and her fetus. Sensor designers need ways of generating and acquiring signals that do not carry the ethical burden of human testing. The development of such a device, as considered in this work, may involve using muscle wire or an inflatable tube as prospective foundations for simulating uterine contraction. After testing the muscle wire, it was evident this approach would not lead to a successful uterine contraction design. Alternatively, an inflatable tube provided a more suitable design to create signals that, to a degree, mimic the contraction of the uterus. The relative intensity of the contraction created by the inflatable tube design discussed here is well-matched to the pressure range of a commercial TOCO. The project also discusses an ECG signal-generation design that can simulate skin measured electrical activity of simultaneous fetal and maternal heartbeats using various equipment. The equipment produces the maternal and fetal electrical signals of 1 and 2 Hz, respectively. Overall, this project resulted in prototypes of the devices that exhibit the required electrical and mechanical signals. These prototypes can be used in ongoing development of a sensor testbed for fetal monitoring.

Table of Contents

Table of Contents (Continued)

Table of Contents (Continued)

List of Figures

List of Figures (Continued)

List of Tables

Chapter 1

Introduction

Pregnancy is a complicated process leading to many changes in the female body, including changes in hormones, and physical body structure, which may lead to other complications. Though many advancements have been made in modern medicine, there remains the possibility for complications during fetal growth. One problem that could occur during the course of pregnancy is fetal hypoxia. Fetal hypoxia occurs when the fetus is deprived of oxygen. If the shortage of oxygen is both prolonged and severe, babies are at risk of being born with a disability, or of dying [1]. Fetal hypoxia is one of many fetal problems that can be corrected by early detection and medicine. Many different technologies exist that could render the occasional fatal outcomes of pregnancy obsolete.

Two of the most important metrics in pregnancy used to assess the health of the fetus are fetal heart rate and uterine contractions. Fetal heart rate measurements refer to the number of fetal heartbeats that occur within a given amount of time. Fetal heart rate monitoring is the surveillance of ongoing human physiology often during or prior to labor, in the assessment of patients with high-risk conditions [2]. Fetal heart rate is an indication of how the fetal heart is functioning. The components of fetal heart patterns are identified by baseline rate, baseline variability, presence of acceleration, presence of deceleration, and types of decelerations [3]. The additional component of pregnancy involves the uterine contraction, which is a muscle contraction of the uterine smooth muscle occurring during the course of a pregnancy. A coordinated series of uterine contractions is necessary for vaginal delivery. At term, the mild uterine contraction becomes gradually more common and intense, transitioning into labor, when uterine forces expand the cervix and push the fetus down the birth canal [4]. Testing these two characteristics on a regular basis will help ensure the fetus and the mother are healthy until the time for the delivery of the baby.

Uterine contraction and fetal heart rate signals can be measured by mechanical, electrical, and magnetic means. There are many devices used for measuring the uterine contractions and fetal heart rate, such as Doppler ultrasound (DUS), tocodynamometer (TOCO), intrauterine pressure catheter (IUPC), and fetal electrocardiograph (fECG) [5]. These devices are required to be tested before becoming commercially viable products. The subjects used for these trials can be either human or animals. These testing phases require an excessive amount of review and associated paper work, are expensive, and may produce risk for the mother and the fetus. Therefore, such a problem creates the need for a tool that could be used by the physician or the device maker to test the uterine contraction and fetal heart rate devices. The device should be able to produce both mechanical and electrical signals of the fetal heart rate and the uterine contraction of a pregnant human woman.

Currently, there is a device on the market called the Victoria S2200 created in 2014. It is a maternal and neonatal birthing simulator created by a company named Gaumard®.This device contains many features such as breathing, obstetrics, circulation, and active birthing baby[6]. This device is able to coordinate the mechanical motion with electrical and/or electromechanical signals using a computer system. It can mimic common signals from DUS, TOCO, and ECG measurements on a computer screen based on a time-coordinated algorithm. However, a few issues make this device not relevant for sensor development and testing purposes. One of the main issues is that this device cannot be used to measure the bio-physiological signals of the body. For example, if the Victoria S2200 were to display the mechanical activity of the uterus, a TOCO would not be able to pick up the signal. Another key issue is the cost of the device, which is approximately $100,000. The next issue is that the displayed signals are a result of the mechanical motion at the time, not the actual measured signals. This device does not contain every bio-physiological signal represented during pregnancy. Another issue with this device is in the way it delivers the fetus, using a piston. Since the Victoria S2200, uses a piston, no electro-mechanical signal representing uterine contraction is produced, therefore a device such as the TOCO cannot pick up the signal. The next few chapters will discuss the apparatus used to measure the mechanical and electrical signals of the uterine contractions and fetal heart rate.

1.1 Devices Measuring Fetal Heart Rate and Uterine Contraction Signals

Cardiotocography (CTG) also known as the electric fetal monitoring is the technical means of recording the fetal heartbeat and the uterine contraction during pregnancy. The objective of this technology is to identify babies who may suffer from fetal hypoxia as well as those who may benefit from a caesarean section or vaginal birth. This device measures the fetal heart externally using either a fetal stethoscope or a DUS machine and the uterine contraction, by a standard TOCO [5]. Although this is a routine part of care during labor, access to such care varies around the world.

One advantage of using CTG is that there are more measurable parameters related to fetal heart rate patterns. Another advantage is the continuous recording of the fetal heart rate and the uterine activity using CTG. This physical record can be examined at any time during labor or subsequently if required. Inversely, one possible disadvantage of this technology is the complexity of the fetal heart rate patterns, which makes standardization difficult. CTG also prevents mobility and restricts the use of massage, different positions, and immersion in water used to improve comfort, control, and coping during labor [1]. CTG is not the only technology used for measuring the bio-physiological signals. There are other methods, which may be more accurate, cheaper, and able to capture these bio-physiological signals more easily.

Figure 1, taken from the open access intrapartum CTG database is a typical recording of a CTG scan during pregnancy. The image displays the uterine contraction and fetal heart rate of real pregnant patients. It is broken into two segments, one representing the fetal heart rate and the other uterine contraction, used together to assess the health of the fetus. Many methods exist that are capable of measuring the physiological signals for a healthy delivery during pregnancy.

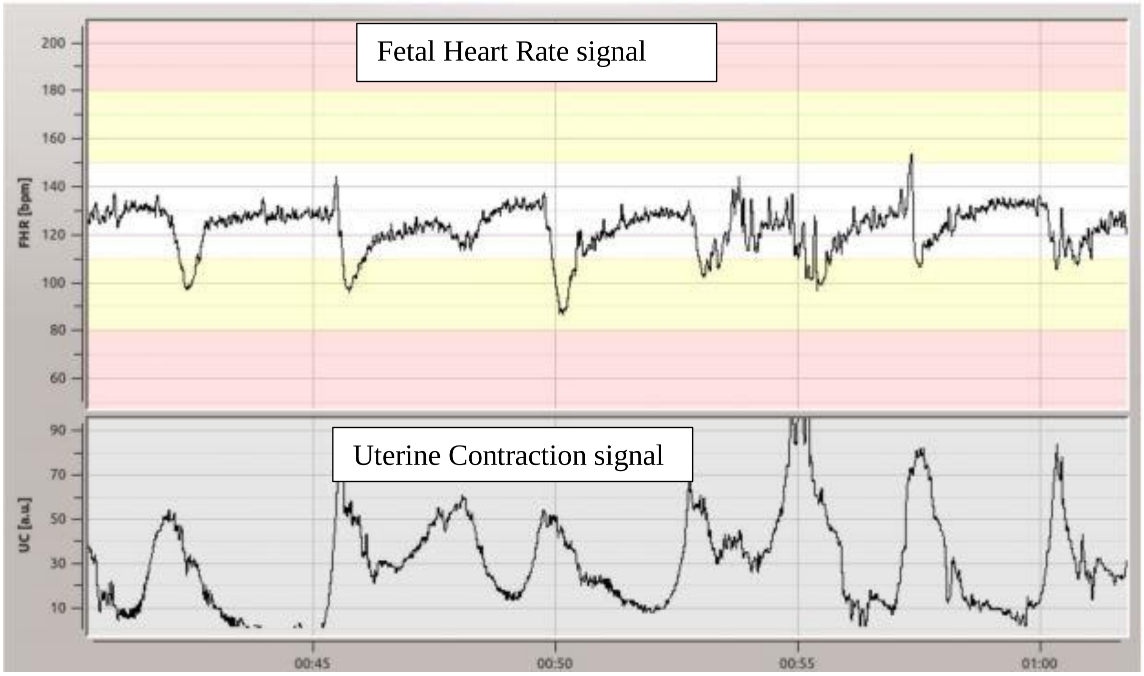

Figure 1. Measured fetal heart rate and uterine contraction using CTG from CTU-CHB Intrapartum Cardiotocography Database [7].

Many devices were developed to measure the bio-physiological signals of the uterus such as the mechanical, and electrical of uterine contractions. The list of devices includes the standard TOCO, pneumatic TOCO, IUPC, Electrohysterography (EHG), Magnetomyography (MMG), and transabdominal Electromyography tEMG. Each device measures the uterine contraction signals using different pressure gauges, transducers, superconducting quantum interference devices (SQUID), and with the use of skin electrodes. Some of these devices may be invasive in nature, while others are non-invasive. The non-invasive methods are most often used during the course of pregnancy to measure the bio-physiological of the uterus since it does not require the membrane to be ruptured. The non-invasive technologies are EHG, pneumatic and standard TOCO, and tEMG. The only invasive method in the list is IUPC.

Figure 2. Illustration of the technologies used to measure uterine contractions and fetal heart rate (a) TOCO, (b) Pneumatic TOCO, (c) IUPC, (d)Magnetomyography (MMG), (e) Electrohysterography (EHG), (f) transabdominal Electromyography (tEMG), (g) Internal Fetal monitor, (h) Magnetocardiography (MCG), (i) DUS, (j) PCG, (k) fECG. References are provided in the accompanying text.

Presently, the most common method of monitoring uterine contractions is with the external TOCO illustrated in Figure 2(a) [8]. One of the greatest aspects of this technology is that it is a non-invasive approach of measuring uterine contractions throughout labor. The TOCO can contain either a centrally located pressure sensitive button or guard ring, and a uniform plunger held against the woman’s abdomen with a band. It is able to detect the change in shape of the abdominal contour [9, 10]. Another function of this device is able to evaluate increased myometrial tension throughout the abdominal wall. In addition, the technology only provides accurate information on the frequency of contractions. It is impossible to extract reliable information on the intensity and duration of contractions, nor on basal uterine tone [5]. This device is the recommended method by physicians for routine clinical use during labor and of measuring the health of a fetus.

Different versions of the TOCO exist which measures the same bio-physiological signals as the standard guard ring TOCO invented by Smyth in the 1950’s. The pneumatic TOCO (pTOCO) exemplified in Figure 2(b) [11] is being introduced as a prototype for monitoring the external contraction pressure. The pTOCO has the same physiology as the standard TOCO but uses a pneumatic pressure sensor instead of the standard electric circuit sensor. Although there are discrepancies in the shape of the pressure-sensitive piston, current commercial instruments retain essentially the same mechanical compliance. The pTOCO has a disc shaped plastic body, where a thin latex free membrane is attached to the surface to attain smoothness that defines the diaphragm compliance [11]. This device is different from the standard TOCO because it is manufactured to be disposable, self-adjusting, smaller, lighter, and low cost. The pTOCO’s self-adjusting and light components allows the pregnant woman to be more mobile and comfortable.

IUPC, represented in Figure 2(c) [12], is the gold standard for assessing uterine pressure and an effective method of monitoring the uterine contraction during labor. However, it is limited by being invasive and that it may be deployed only following the rupture of the uterine membrane [13, 14]. It works by directly measuring pressure within the amniotic space using a transducer, which allows for the quantification of contraction strength. The transducer is inserted inside of the amniotic fluids of the uterus, via the cervix. The IUPC provides quantifiable information on baseline tone, duration, amplitude, contraction and relaxation time [15, 16]. Complications such as fetal injury, placental hemorrhage, uterine perforation and intrauterine infection are rare but have may occur during the insertion of transducer [5]. Although the risk may be a rare occurrence, it still proves to be a serious matter when it occurs.

MMG, shown in Figure 2(d) [17], is a technique used to measure the magnetic activity on the surface of the abdomen. The magnetic activity is a result the collections of action potentials generated and propagated in the uterine muscle. The recording of the magnetic fields, produced by the electrical current occurring in the uterine muscle, is done using arrays of SQUIDs for reproductive assessment [18, 19]. These currents can be detected by a measurement of potentials inside or on the surface of the body. The physics of electromagnetism predicts the flow of current will result in a magnetic field [19]. The MMG recordings have important properties such as independence of tissue conductivity, detection of the signal boundaries of the skin without any contact and is independent of references [18]. MMG is a novel technique and is not frequently used by physicians during labor.

(EHG), portrayed in Figure 2(e) [16], is a non-invasive method of measuring the electrical activity of the uterus. The aim of this technique is to provide information on the uterine activity during labor and throughout pregnancy. EHG is accomplished by the measurement of action potential of the myometrium cells by placing electrodes on the maternal abdomen [20, 21]. During an EHG reading, a couple of components can be distinguished which are fast and slow waves. Many different noise signals such as the maternal ECG and mechanical artifacts are present in the abdominal wall. [20]. These signals make it almost impossible to get a useful recording of the electrical activity of the fetus's heart. However, there are ways of acquiring a good signal through filtering the signal.

Uterine contractions are generated by the electrical activity originating from the depolarization and repolarization of the billions of smooth muscle myometrium cells. [22]. Electrical activity of the myometrium can be monitored by a device called tEMG depicted in Figure 2(f) [23]. There are different ways of performing a uterine/transabdominal EMG on a pregnant woman. Once such way is by having two pairs of $AgCl_2$ electrodes applied to the abdominal wall. [24]. Another way is by using electrical uterine myography (EUM), which uses 9 electrodes placed on the maternal abdominal surface to evaluate uterine contractions [25]. These methods are able to evaluate the frequency, duration, intensity, and time to peak of the uterine contraction. A downfall of this technology is that mechanical artifacts, maternal ECG affect the signal.

Many devices also exist that measure the bio-physiological signals of the fetal heart during pregnancy. There are the non-invasive techniques, which uses either transducers or electrodes to measure the bio-physiological signal on the outer surface of the body. On the contrary, there are also invasive methods, which require inserting the devices through the membrane. The devices below include the internal monitoring devices, fetal PCG, MCG, DUS, as well as the fetal ECG. The non-invasive devices include MCG, DUS, fetal ECG, and fetal PCG. The invasive method is internal monitoring.

The internal monitoring represented by Figure 2(g) [26], is done using disposable fetal electrodes, connected to the fetal scalp. To accomplish such a measurement, the cervix must be dilated 2 - 4 cm and the membrane must be ruptured [5]. This method is invasive, therefor conducted during labor. Since it is an invasive procedure there are risks of infection to the mother and fetus at the application site. The scalp electrode acquires the fetal electrocardiogram, which is used to evaluate time intervals between successive R waves. The R wave is the biggest peak of the QRS wave complex [5]. This technology is one of the most precise ways of evaluating the intervals of the heartbeat. The internal fetal heart rate monitor provides better signals tracings of the heart than any other external monitoring device.

MCG, characterized by Figure 2(h) [27], is a non-invasive technique for contactless surface mapping of the magnetic fields generated by the electrical activity of the heart [28]. The MCG technique shares similarities with the (ECG) and MMG. The recording of the cardiac magnetic field is performed with an external sensor that is not exposed to the body [29]. Similar to the MMG, the MCG also consists of an enhanced detector of the magnetic fields called SQUID. This device measures bio-magnetic signals, which are very weak and can be detected by the most sensitive magnetometer. The problems with this method are very similar to the ECG, though the acquired R–R time intervals and the corresponding FHR values are very accurate and suitable for deriving parameters [30].

DUS, denoted by Figure 2(i) [31], is the most regularly used non-invasive tool providing accurate and vigorous information of the fetal heart rate. This test uses high frequency sound waves to measure and detect the movement of blood in vessels. During the assessments, the ultrasound transducer pulses at 2 MHz from the abdominal surface toward the fetus. Doppler Ultrasound works by using the reflected and received ultrasound signals from the transducer. The transducer is placed on the maternal abdomen via the support of an elastic band around the abdomen, directed at the fetal heart. The frequency of the ultrasound wave reflected from moving parts, like valves of the fetal heart, is shifted in agreement with the Doppler Effect. The echoes received by the transducer are demodulated to obtain differential frequencies describing the movements within the ultrasound beam [20].

PCG, represented by Figure 2(j) [32], detects the sound of the heartbeat using an amplifying microphone. The opening and the closing of the fetal heart valves produce the fetal PCG signals. It is non-invasive and captures the PCG signal with a small acoustic sensor placed on the mother's abdomen [33]. However, noisy environments affect PCG and the ideal form of the sound signal cannot be measured due to disturbances [34]. Sources of disturbance from the fetus include movement of limbs, rotation of body, hiccups, breathing movements, and disturbances from the mother due to her heart sound, breathing, digestive organs and muscular movements. [30]. The small fetal heart produces low intensity signals and the frequency band is very narrow because of the damping of the maternal tissues. The PCG detects different sounds labeled S1, S2, S3, and S4.

A well-known method of measuring the electrical activity of the heart is called ECG, and is indicated by Figure 2(k) [35]. This method uses silver/silver chloride electrodes to measure the electrical activity. Similar to an adult ECG, the fetal ECG displays the P, QRS, and T waves corresponding to the electrical events in the heart during each beat. The P waves represent atrial contractions, QRS signify ventricular contraction, and T waves characterize the ventricular repolarization [36]. The fetal ECG is the least frequently used non-invasive method of measuring the fetal heart rate. This device uses electrodes connected to the abdominal surface of the mother. One of the main reasons for its limited use is due to its complex signal processing. The fetal ECG also takes into account the mother's ECG, which overshadows the fetal ECG. One other reason for its limited use is that the signal quality is dependent on proper placement of the electrodes. Although fECG has some setbacks, two benefits are its low cost and passive measurement technology [34].

Table 1 offers a brief description of the advantages, disadvantages and limitations of some of the devices used to measure the bio-physiological signals of the uterus and heart. Table A1 found in Appendix A discusses the advantages, disadvantages and limitations of the devices in more details. The ideal choice for measuring the mechanical activity of the uterus is the TOCO. The TOCO is non-invasive and provides precise information on the frequency of contraction. Likewise, the best means for measuring the electrical activity of the fetal heart rate is the non-invasive, low-cost method called ECG. The other methods were not selected because the advantages mostly outweigh the disadvantages. For the DUS method, overexposure to the ultrasound wave could prove to be detrimental to the health of the fetus. MCG and MMG devices and examination are both expensive. The IUPC and internal fetal monitoring are invasive methods. The PCG has difficulty extracting information and is extremely susceptible to noise.

Table 1

Advantages, disadvantages, and limitations of the devices used to measure the bio-physiological signal of fetal heart and uterus

Devices	Advantages	Disadvantages	Limitation
TOCO	• Non-invasive Provides precise info on frequency of contractions	• Not highly reliable for duration and intensity	• Depends on proper placement Not disposable
pTOCO	• Lighter Disposable	• Need for a belt to hold transducer in place	• Not available
IUPC	• Gives decent info on duration, amplitude and contraction.	• Invasive • Increases rate of infection.	• Used only during labor.
EHG	• Laplacian potential improves the spatial resolution	• Obtrusion from bipolar and monopolar recording	• Bipolar and monopolar have low spatial resolution
CTG	• Less instances of seizures in newborns	• High sensitivity to noise • Frequent shifting	• Accuracy • False positives Uncomfortable
MCG	• Non-invasive • Contactless	• Expensive • Sensitive to metal objects and pacemakers	• Not portable • No bedside availability
ECG	• Non-invasive • Inexpensive	• Restricts body movement	• False positives and negatives
DUS	• Non-invasive	• Effected by movement • Prone to signal loss	• Requires signal modulation for good recording
PCG	• Cheap Non-invasive	• Difficulty extracting information • Susceptible to noise	• Prone to noise such as maternal breathing, fetal and maternal heart contraction
CTG	• Less instances of seizures in newborns	• High sensitivity to noise • Frequent shifting	• Accuracy • False positives • Uncomfortable

1.2 Motivation/Objective

Section 1.2 describes the different technologies used to measure the physiological signals that occur during pregnancy. The thesis will discuss the "pregnant woman model" developed for the testing of devices such as ECG and TOCO. The objective of this project is to produce a device that displays both the mechanical activity of the uterus and the electrical activity of the fetal heart. One of the best ways to guarantee that the product fits the target market is to test the device with the subject group. A car for example before going on the market goes through many rounds of safety testing. To ensure safety of the driver and passengers, humans would be the ideal subjects for safety testing. However, it is dangerous to subject humans to such a test. Therefore, crash tests dummies were invented to replace human beings with similar anthropometry. Consequently, this will give the car manufacturer an idea of what will occur to a human being in the case of an accident and make the car safer.

Similarly, developing a device that does the same job as the crash test dummy, which takes the place of a pregnant human as a test subject would be optimal. An existing technology may always improve due to the progression of knowledge. The advancement in medical technology warrants biomedical devices measuring the bio-physiological signals of the body to be refined. This could entail a change in hardware, software, sensors and other such things. For instance, the development of a new sensor would require a test subject such as a pregnant woman to provide the bio-physiological signal for the prototype sensor to measure. Nonetheless, it may prove risky to use a human being therefore there is a need to develop a testbed that can model the signals that are generated by the fetus and mother during pregnancy. This device will share similar bio-physiological signals as a woman during gestation. The intention is to provide bio-physiological signal such as mechanical, electrical, and other signals for developing the devices to be tested on. Although the Victoria S2200 is a lifelike pregnancy simulator and is considered the state of the art, it does not provide the ability for devices to measure the biological signals created by the model.

This project is the first of its kind at Rowan University; therefore, some groundwork will need to be done to create such a device. Due to the novelty of this venture, the projected task of this thesis is to introduce the idea and preliminary design. All of the results found during the advancement of this research, aided with the progression of the project. This project began in the spring semester of 2018 and concluded in the Fall of 2018. The main goal of the project is to create a device, whose signal is similar to that of the uterus and heart. The first part was to understand the way the uterus and heart functions. The next step was to understand the bio-physiological signals of the body. Following that was to understand how the devices are used to measure these signals. To be able to create the devices, all of these pieces are relevant.

Given that the goal is to develop an electro-mechanical device that exhibits the bio-physiological signals of the body during pregnancy, a few ideas come to mind of how to achieve it. First, creating the mechanical activity of the uterus will require a device or mechanism that is able to contract and expand. One of the devices capable of such a feat is using muscle wire. Another example of a device that is able to contract and expand is an inflatable balloon. Either of these ideas may be able to provide the mechanical activity of the uterus with some ingenuity. Another goal of the project is to develop a device exhibiting the electrical activity of the fetal heart. This can by using a software program named LabVIEW and its hardware counterpart called the Data Acquisition Device (DAQ).

1.3 Overview of Thesis

The key contributions will be discussed in the subsequent chapters. Chapter 2 will discuss the mechanical activity of the uterus as well the way muscle wire would be used to represent the signal of the uterine contraction. Due to the failure of muscle wire, Chapter 3 will discuss an alternative way of maintaining the mechanical activity of the uterus using inflatable tubes. Manufacturing the device exhibiting the mechanical activity involves doing analytical calculations, and COMSOL simulations to figure out the best polymer to use for the inflatable tube. In Chapter 4, the fetal heart rate and the method of producing the electrical activity of the heart will be discussed. Lastly, Chapter 5 will contain the overall conclusion, limitations, and future works.

Chapter 2

The Application of Muscle Wire in Simulated Actuation of Uterine Mechanical Activity

2.1. Introduction

The purpose of this chapter is to investigate how muscle wire can contribute to replicating the mechanical contraction activity of the uterus. Muscle wire is also known as flexinol, nitinol, Ni- Ti alloy, and shape memory alloy. It is an equiatomic alloy of the transition metal series nickel (Ni) and titanium (Ti) [37]. When heated, this wire acts similarly to the muscle in the body it contracts, so its main purpose in the present project is to actuate contraction of an enclosure simulating a woman's abdomen during uterine contraction.

Although thin and lightweight, muscle wire can lift many times its weight and is do 100 times more work per cycle than the human muscle. This material is easy to use, small, operates silently, has a high strength-to-weight ratio, and is easily activated using AC and DC power. This wire is well-known for contracting when electric current or heat is applied and expanding when cooled. Muscle wire is able to expand and contract due to its combination of crystal structures from the nickel and titanium metal [38]. The material can be plastically deformed, and then restored to the original shape by heating it above the characteristic transition temperatures [39]. This is an important aspect, as the uterus contracts due to the firing of the uterine smooth muscle cells and returns to its original state after contractions end.

Figure 3 roughly represents the shape of a woman's abdomen during pregnancy and motivates the present discussion. The notion for the design was to construct a prototype mechanical uterus by using the muscle wire as the contraction agent. In principle, a whole network of muscle wires attached at different angles could be used to simulate an evenly distributed contraction; depending on the approach, more complex space-and-time varying contractions could also be accommodated. Within the ultimate sensor testbed prototype, there would be a device used to control the activity of the muscle wire such as a power supply. Figure 3 is an example of the arrangement of the muscle wire within the structure to exhibit the mechanical activity of the uterus. Figure 3 represents is an example of the arrangement of muscle wire within the structure to exhibit the mechanical activity of the uterus.

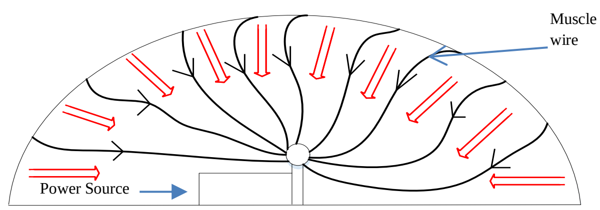

Figure 3. Schematic of device use to represent the mechanical activity of the uterus using muscle wire.

2.2. Uterine Contraction Background

In prearation of creating a device that measures the mechanical activity of the uterus, it is important to know the basic physiology of the uterus. The uterus contains three layers with form the uterine wall. The three layers from innermost to outermost are the endometrium, myometrium, and perimetrium. During pregnancy, the endometrium is responsible for accommodating a developing baby. The myometrium consists of uterine smooth muscle cells known as uterine myocytes, whose main occupation is to induce uterine contractions. The perimetrium is the membrane that surrounds and protects the uterus [40]. From a mechanical standpoint, myometrial behavior is the most important behavior to model.

The contraction of the myometrium within the uterus is not purely a mechanical occurrence. The process transpires simultaneously with the electrical activity of the uterus. A mechanical contraction is a consequence the excitation and propagation of electrical activities in the uterine muscle, and appears in the form of an intrauterine pressure increase [41]. Uterine contractions occur throughout the menstrual cycle in the non-pregnant state and throughout gestation. The four parameters that change under numerous pathophysiological or physiological circumstances during gestation and menstruation are the frequency, amplitude, duration, and direction of propagation [42]. At full term of conception, the human uterus measures 40 - 42 cm in the axial direction (fundal height) and 35 - 37 cm in the transverse directions(fundal width) [43].

The uterine contraction causes the cervix to thin and widen, and helps the baby descend into the birth canal. Formally, the definition a uterine contraction is a tightening or hardening of the abdomen throughout pregnancy. Therefore, the uterine contraction signal is a very good way to evaluate the health of the fetus and mother. Uterine activity progressively increases until the fetus is delivered. During labor, intrauterine pressure rises to 60 - 100 mmHg and is concurrent with contractile activity of the myometrium [44]. The mechanical activity of the uterus is measured using different methods, the most widely used is a non-invasive method called the TOCO. During labor, physicians use the invasive method called IUPC to evaluate the fetal health.

2.2.1. Limitation of uterine studies. Without the approval of the Food and Drug Administration (FDA), experiments on the mechanical activity of the uterus of a human being cannot be achieved. Therefore, there is limited experimental data to characterize the mechanical response of the uterine myometrium. The pregnant uterus cannot be measured directly, therefore it is restricted to minimally invasive measurements and a small number of samples [45]. Therefore, it is difficult to acquire experimental data that are pertinent and adequate in number. This issue demands the creation of a method of exhibiting the mechanical activity. Presently, there are not many methods of directly monitoring the mechanical activity of the human uterus. Techniques such as computational/mathematical and animal models have been used to replace of human beings. Although some human and animal physiology is nearly the same, animal models are not always appropriate, as they differ from human pregnancy in aspects such as tissue organization and overall structure, among others. Regardless, these offer an overall understanding of how the uterus performs during the gestation and non-gestation phases. Animals such as rats, dogs, sheep, and monkeys have been studied for such experiments. Instead of human trials, the best means of obtaining data on mechanical activity of the uterus is with the use of computational/mathematical models of pregnant human beings.

Cochran and Gao show one example of a study simulating the mechanical activity of the uterus. In the article, uterine contractions were simulated to measure the impact that a ±3% change in the mechanical and electrical properties has on peak intrauterine pressure and the duration of peak pressure. The peak pressure was affected by the changes in one mechanical property, the maximum stress generated from cellular contraction [46].

Bursztyn et al and Tong et al conducted two similar studies on the uterine smooth muscle cell. The authors create a model of the excitation-contraction in a uterine smooth muscle cell. The models describe the ways that the cells contract. During the contraction, the smooth muscle cell shortens and exerts a force on the neighboring cells [47, 48]. It shows that the uterine contraction is caused by the uterine smooth muscle cell and occurs at the cellular level. They conducted these models to get insight on how the uterine muscle cells induce uterine contractions.

La Rosa et al modeled uterine contractions to interpret the mechanical and electrophysiological aspects of the uterine contraction measurements and developed a more accurate method for predicting labor. When it comes to uterine contraction, both the mechanical and electrical aspects are involved, since the electrical activity is the mechanism that triggers the mechanical activity [41]. This study aided in mathematically modelling the contractions occurring during pregnancy. It is a step in the right direction to understand the contractility of the myometrium in understand the mechanism of labor.

Sharifimajd simulated human uterine contraction by implementation of a coupled model in a finite element scheme, and the intrauterine pressure was evaluated as a response. This model gives a better understanding of the intrauterine pressure of the uterus during pregnancy [45].

Other models have been created of different aspects of the mechanical activity of the uterus using computational/mathematical simulations. Given these models, one can now gain insight of the mechanical activity of the uterus. With this information, it would be possible to create such a device, a physical model with the purpose of exhibiting a signal comparable to the contraction and relaxation of the uterus during pregnancy and labor. The first attempt at creating a device that exhibits the mechanical activity of the uterus is using muscle wire.

In particular, Ni-Ti shape memory alloys (SMAs) have found many biomedical applications due to their excellent biocompatibility. Ni-Ti SMAs also show excellent MRI compatibility, and resistance to kink and corrosion. All of these properties make muscle wire a good choice for many biomedical applications such as guide wires, drug delivery systems, self-expanding stents, implantable devices, catheters, atrial occlusion devices, and thrombectomy devices [49]. One such application is in the design and fabrication of a three-finger prosthetic hand using shape memory alloy muscle wire. In this work, Simone et al. focus on emulating the biological structure of the human hand and the natural muscle tendon arrangement in developing a new biomimetic prosthetic gripper. The use of thin wires (100-μm diameter) allows for high cooling rates and therefore fast movement of each finger. Grouping several small wires mechanically in parallel allows for high force actuation [50]. This is similar to the purpose of using the muscle wire to exhibit the electromechanical signal of the uterus.

Another use of Ni-Ti alloy in the biomedical field is in cardiovascular applications. By Stepan et al where nitinol is used to create a heart valve that is less prone to clotting with improved longevity. A butterfly valve was fabricated using a single elliptical piece of thin film Ni-Ti and a scaffold made from Teflon tubing and Ni-Ti wire. To determine the material's in vivo biocompatibility, thin film nitinol was implanted in pigs using stents covered with thin film Ni-Ti [51].

Erkan Kaplanoglu used the ring and pinky fingers are selected for shape memory activation due to their lower degree of movement during grasping configurations. The fingers' tendon system is based on muscle wires that form artificial muscle pairs for the required flexion and extension of the finger joints. These fingers had four degrees of freedom, such that three were active. An experimental setup was developed to assess the performance of the ring and little fingers after the device was manufactured [52]. Overall, muscle wire is a versatile metal used many applications. Nitinol alloys are cheaper to produce, easier and safer to handle, and has better mechanical properties compared to other existing shape memory alloys.

2.3. Experimental Setup

The materials and equipment used during this experiment are muscle wire, Hewlett-Packard E3632A power supply, alligator clips, support stand, weights, and a measuring apparatus, illustrated by Figure 4. Alligator clips needed to be connected to both sides of the wire to ensure the flow of current from both ends. The purpose of the mass is to find out how much force the muscle wire can displace. The power supply produced the current for heating the muscle wire. The test that will be conducted for the mechanical properties is a uniaxial stress-loading test where one end is fixed, and the other end contains a load. The muscle wire is suspended from the stand using a clamp in the longitudinal direction and different masses such as 10 g, 20 g, and 30 g were placed on the muscle wire. The measuring tape was fixed behind the wire to measure the displacement caused by the flow of current through the muscle wire.

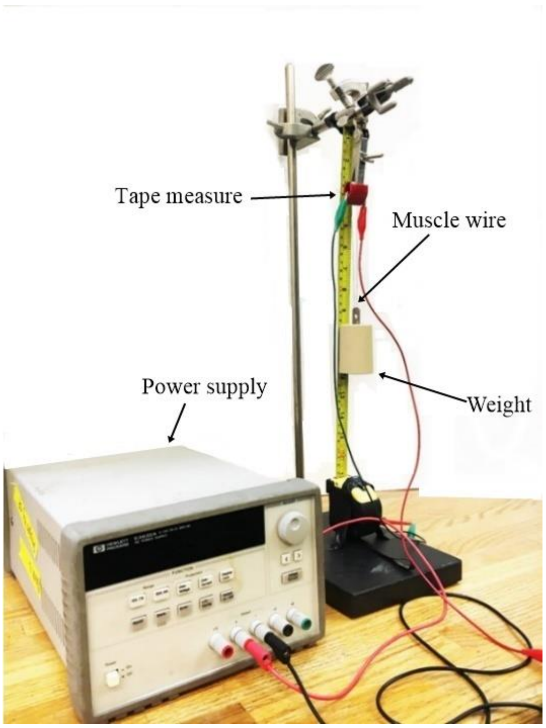

Figure 4. Experimental setup for muscle wire.

2.4. Procedure

Table 2 displays the different technical characteristics of muscle wire used in the experiment, where D is the diameter, and R is the resistance. Such methodological attributes include resistance, pull force, deformation, applied curent for 1 second contraction, and cooling time for low temperature wire. The wires in Table 2 will be used in the experiment to simuate the actuation of the uterine mechancial activity.

Table 2

Characteristics and properties of muscle wire used in experiment [53]

D (mm)	R (ohms/meter)	Pull Force (Newtons)	Cooling deformation Force grams	~ current for 1 s contractions mA	Cooling time 158°F, 70 ℃ "LT" Wire (s)
0.13	75	223	89	320	1.6
0.31	12.2	1280	512	1500	8.1

Prior to using muscle wire to simulate uterine contraction, it needs to be tested. The test will help in determining if muscle wire is a viable option to produce the mechanical activity of the uterus. Two diameters of muscle wire were used during this experiment, 0.13 mm and 0.31 mm as displayed in Table 2. The difference in diameter is important because of the difference in mechanical properties of the wire. The smaller wire accounts for a faster cooling rate than its larger counterpart does. However, the smaller wire may not be able to withstand as much power as the thicker wire. The first wire that was tested was the 0.13 mm wire. The second wire of 0.31 mm was tested in the same manner. The amount of potential used was dependent on the size of the wire as well as how much mass is loaded on the wire.

2.5. Results and Discussion

After observing the 0.13 mm muscle wire, the wire did not seem to be able to withstand an adequate load due to its size. After applying the 10 g mass to the wire and supplying the muscle wire with some voltage, the wire began to burn. The maximum potential applied before the wire started to burn was approximately 2 V. Due to the wire burning during the experiment, no displacement occurred. Since this wire cannot displace much weight and the power of 2 V destroys the wire, the 0.31 mm wire was used instead. The bigger wire of 0.31 mm allowed for further experimentation. The intended plan for this wire was to observe the maximum amount of weight that would produce a significant displacement when current is running through it. The amount of mass used for this experiment started with a 10 g mass. The intention of this experiment was to observe the maximum load that would result in a sizable deflection using a range of masses. After the 30 g mass, no noticeable deflection occurred.

One constraint of this experiment is the amount of power that the wire could handle. The first experiment done was using a 10 g washer with a potential of 2 V. Voltage was changing to find out how much displacement can occur with an increase in potential. The highest voltage that could be achieved before the muscle wire started burning was 5.5 V. This same case was applied for the 20 and 30 g masses.

Figure 5 represents the displacement across the potential graph of the 10, 20, and 30-gram masses of the 0.31 mm muscle wire. The importance of this graph is to show the impact of different masses on the muscle wire and the change that occurs when a heat source is present. A higher mass results in a higher rate of change in displacement, where the rate of change is dependent on voltage. To summarize, a higher mass requires a higher voltage for greater displacement. The 10 g weight seems to exhibit a more positive deflection due to its size. Based on observing the trend of the line, if the wire permitted more current to flow through, a more positive displacement would be achieved. The 20 g weight shows the same type of inclination but seems to be reaching its maximum peak at 5 V. If the trend continues, the graph for the 20 g mass would begin to either plateau or plummet. The 30 g weight has a different behavior, as from the beginning it is consistently leveled, where minimum displacement occurs. With the increasing voltage, the displacement stays under 2 mm for the 30 g weight. Based on the properties and the test conducted on the muscle wire, in theory the muscle wire may have the ability to simulate the mechanical activity through contraction with an induced current.

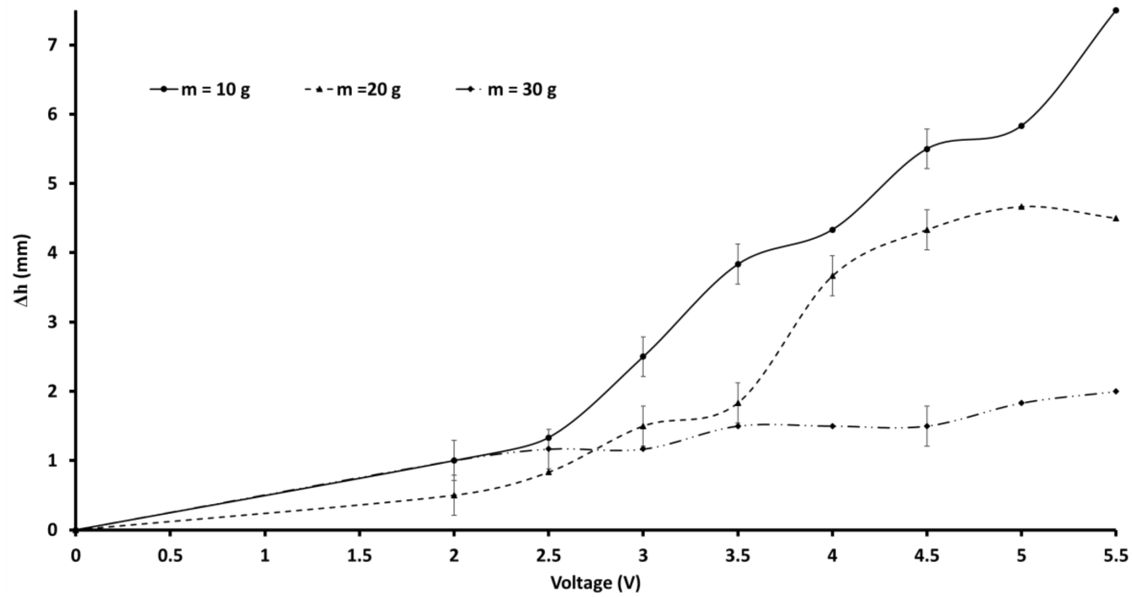

Figure 5. Muscle Wire Displacement vs Voltage.

There are a few limitations in using muscle wire to actuate the mechanical activity of the uterus. First, limited resources were available to allow such a device to be created. The pregnant uterus measures 40 - 42 cm in the axial direction and 35 - 37 cm in the transverse directions [44]. With this information, the surface area of the pear-like structure could be calculated. The pear shape could be represented as a rectangle to give a crude estimation of the surface area of the uterus.

To calculate the amount of wires needed to actuate the uterine contraction, the surface area of the uterus and the pressure on the uterus are essential. The calculation of the pressure and the area will result in a representative force for the contraction during pregnancy. The force of a single muscle wire was found by using the amount of mass the muscle wire can displace against gravity for the uniaxial test. The surface area of the uterus is the product of the length and width of the uterus, 1477 cm^2 or 0.1477 m^2. The task now is to find the amount of wires needed to produce 80mmhg = 10.67 kPa [44] of pressure over the surface area of 0.1477 m^2. The pressure of 10.67 kPa is the average pressure caused by contraction occurring in the uterus, measured by the IUPC. This could be realized by first multiplying the pressure of 10.67 kPa by the surface area of 0.1477 m^2 to yield 1.6 kN of force.

During the testing of the muscle wire, the limit of the amount of mass that a single strand of muscle wire could displace was found to be 30 grams. To get the force on the muscle wire, the mass in kg was multiplied by gravity giving a 0.3 N force. After calculating the force of contraction of the uterus of 1.6 kN and the force of the muscle wire of 0.3N, the amount of wires needed can be done by taking a ratio the forces. The ratio of the forces yields 5226 muscle wires required to actuate 10.67 kPa over a surface area of 0.1477m^2. Having to use 5226 wires is inefficient and not financially feasible. Secondly, the amount of power needed to actuate these wires may also be a limitation. With an applied voltage, there is a corresponding current, which can be used to calculate the power. The maximum power applied for the actuation of the wire was 13 watts. To actuate 5226 wires, approximately 68 kW will be required. This is an irrational amount of power needed to actuate the mechanical activity of the pregnant uterus using muscle wire. Third, acquiring a biocompatible material such that the current does not produce a fire upon activation is another limitation. To put this into perspective, the amount of power needed to run the 5226 wires is equal to the amount of power needed to run approximately 68 refrigerators of 1000-watt simultaneously.

2.6. Conclusion

Although the muscle wire could be a method to simulate the mechanical contraction of the uterus, it has a few drawbacks. The preliminary experiments conducted on the 0.13 mm diameter and the 0.31 mm diameter wires, along with the mechanical properties of the wire supported the notion that it is possible. However, upon further investigation of the surface area of the uterus during the late stages of pregnancy, which is around 0.147 m^2, 5226 wires will be essential to producing the mechanical activity of the uterus. In parallel, the amount of power needed to actuate all of these wires is approximately 68 kW. As a result, the consensus was made that pursuing this idea was no longer a viable option. The amount of power and muscle wires is unreasonable and inefficient. Consequently, another method was devised to exhibit the mechanical activity of the uterus. This idea will involve using an inflatable structure as a representation of the mother’s abdomen. As will be shown, the inflatable tube is a more practical avenue to pursue.

Chapter 3

Mechanical Design of Pregnant Woman Model Using Inflatable Tube as Actuating Source

3.1. Introduction

A feasible option for producing a device that exhibits similar physiological signals to the uterus is using inflatable objects, as shown in Figure 6. A collection of inflatable objects is evenly distributed within a soft structure. They can be inflated and deflated consecutively to provide expansion and contraction motions. An inflatable object has the ability to inflate with the use of a gas, usually with pressurized air. The object goes back to its original shape once deflated, because it depends on the presence of the pressurized gas to maintain its size and shape. This seems to be a viable option in simulating the uterine contraction occurring during gestation.

The purpose of this chapter is to discuss an alternative method in producing the mechanical activity of the uterus. It is well known that an inflatable tube has the capacity to expand and compress using pressurized gas or a mechanical pump. There are not any known studies using inflatable tubes for the contraction of the uterus. However, a gastric balloon is an inflatable medical device this is placed in the stomach to aid in weight loss. Since the inflatable tube is an option, it is possible to make a computational model using COMSOL and solve analytically for thin walled pressure vessels to analyze the deformation due to pressurized air. This will assist in the creation of a device that will exhibit the mechanical activity if the uterus. The calculation and COMSOL simulations are accomplished to validate that the radial displacement of an inflatable tube is similar to that of the uterus.

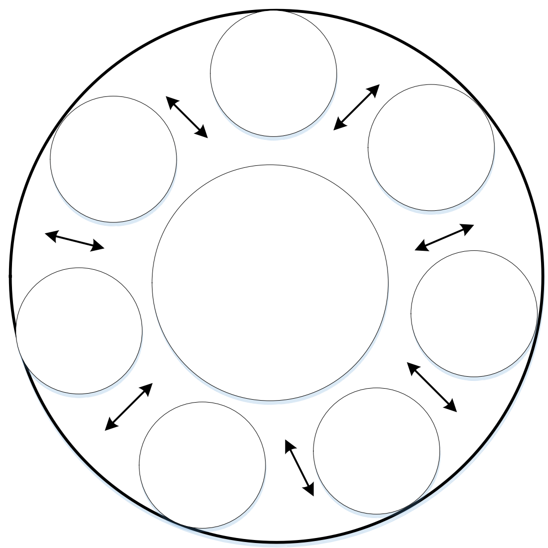

Figure 6. Schematic of an inflatable object with contraction and expansion capability.

3.2. Calculation of Thin Walled Cylinder

Preceding the simulation of the tube using COMSOL, a calculation can be made to estimate the displacement occurring within a thin walled cylindrical tube. The calculation can be used to validate the COMSOL to ensure comparable results. The equation for the displacement of a thin walled cylinder is found by using the equation below [54]:

$$\delta r = \frac{Pr^2}{tE}\left(1 - \frac{\nu}{2}\right)$$

where, δr refers to the radial displacement, P refers to the pressure of the uterus during labor and the pressure flowing through the tube, r is the outer radius of the cylinder, t is the thickness of the cylindrical wall, the ratio $\frac{r}{t} \geq 10$, ν is the Poisson's modification, and E is the Young's modulus of the material. The equation for a thin walled cylinder is bounded by assumptions; which include the radius of the cylinder as well as the pressure. These assumptions themselves are bounded by limitations. They tend to be linearized for small defections relative to the total radius of the total length. The average intrauterine pressure of 80 mmHg (10.67 kPa) was chosen as the intensity of contraction for the simulation and calculation. A few materials were selected to determine the material best suited for displaying the mechanical activity of the uterus. The materials are poly (methyl methacrylate) (PMMA), polydimethyl-siloxane (PDMS), silicone rubber, soft poly-vinyl chloride (PVC).

Table 3

Calculation of displacement using equation

Material	Pressure (P) Pa	Radius (r) mm	Thickness (t) mm	Young Modulus (E) MPa	Poisson's ratio (ν)	Deflection (δ) mm
PMMA	10665.78	180	5.8	3×10^3	0.4	0.016
PDMS	10665.78	180	5.8	0.75	0.5	59.58
Silicone rubber	10665.78	180	5.8	25.5	0.5	1.75
Soft PVC	10665.78	180	5.8	35	0.5	1.27
Steel AISA 4340	1.2×10^6	62.5	5	200×10^3	0.3	0.0040

Table 3 describes the calculations to determine the most appropriate material for the experiment. The materials labeled on the table were selected based on their availability, elastic modulus, and their prevalence in the COMSOL software. Steel AISA 4340 was used as a standard material for validation purposes, due to its well-known properties. This was done to assure that the calculations and COMSOL results are close in proximity. The components for the calculation was are pressure, radius, thickness, Young's modulus, and the Poisson ratio.

Thickness is another important aspect of the uterus. The thickness of the cylindrical model is the difference between the outer and inner radii, which is a representation uterus where the fetus is located. The uterus gets significantly thinner as the pregnancy progresses. The thickness of the uterus is found by averaging 4.5 mm to 7.0 mm [44]. The equation above involves the radius of 180 mm, where the diameter is 360 mm. Using the equation above, the displacement of each material came out to be 0.016 mm, 59.58 mm, 1.75 mm, 1.27 mm, and 0.0040 mm for PMMA, PDMS, silicon rubber, soft PVC and steel, respectively. These calculations provide answers that could be used along with the COMSOL for assessing which material would be suitable for the mechanical activity of the uterus.

3.3. COMSOL Simulation

The software used to simulate the uterine contraction is a user-friendly computational software called COMSOL. The next step in manufacturing the uterine contraction device is to simulate the performance of the device using a representative model. The simulation encompasses different characteristics such as material and specification. Therefore, one of the ways to simulate is to use the idea of an inflatable tube to assist in the representation of uterine contraction signals in the uterus. The COMSOL simulation uses the Navier-Stokes equation among other components to calculate the displacement.

3.3.1. Procedure. In COMSOL, a simulation of the displacement occurring within a cylindrical tube was completed. Air pressure was used as the material flowing through the inflatable tube. The tube is pinned on both sides to stop air from escaping, on one side by the air pump and the other by a cap. This test was done to see how much a tube could contract using different elastic materials. The same materials PMMA, PDMS, soft PVC, silicon rubber, and steel will be used in the COMSOL simulation. Other considerations should be the geometry of the tube including the length, inner and outer diameter of the tube.

Another important aspect to consider is the physics used to simulate the tube. The two types of physics used in such a problem are the fluid flow and structural mechanics physics. Under the single-phase fluid physics, the interfaces to choose from are creeping flow, laminar flow and turbulent flow. The type considered for the simulation is laminar flow. Laminar flow is used to compute the velocity and pressure fields for the flow of a single–phase fluid in the laminar flow regime. A flow will remain laminar as long as the Reynolds number is below as certain critical value. The next type of physics is the structural mechanics, which contains physics interfaces for analyzing deformations, stresses, and strains in solid structures.

Under the structural mechanics option, the chosen interface was solid mechanics intended for general structural analysis of 3-D, 2-D, and 2-D axisymmetric bodies. The solid mechanics interface is based on solving Navier's equations, where results such as displacements, stresses, and strains are computed. All of the simulations were done using a 2-D axisymmetric space. 2-D axisymmetric models represent a slice of a 3-D model, which if revolved around the y-axis of a Cartesian coordinate system would become the original 3-D structure. The purpose of choosing a 2-D asymmetrical space is because it is much simpler and is able to give the acquired displacement. For the 2-D axisymmetric model two rectangles were used, one to represent the "inner radii" and the other to the "outer radii represented in a 3-D model. During the simulation, the 3-D model has a tendency of being more complex, harder to mesh, and can take a lot of time to compute. Therefore, the simulations were executed using 2-D axisymmetric space.

3.3.2. Results: In Table 4, the pressure chosen was based on the intensity of the average contraction women during labor feel of 10.67 kPa. The chosen physics is laminar flow for all simulations. The study for all of these simulations were stationary based since the field variables do not vary over time. The length was chosen based on the size of the uterus close to the end of the third trimester. The length used for the simulation is 420 mm. The purpose of the inner and outer diameter is to have a value for the thickness of the uterus of 5.8 mm. This represents the average thickness of the uterine wall within the uterus of the uterus. As the pregnancy progresses the mother's uterus gets thinner due to the fetus growth. After assessing the parameters, each of the materials provided on table 4 each resulted in a displacement. The PMMA had a displacement of 0.0043 mm, PDMS with 15.6 mm, silicone rubber of 0.23 mm, Soft PVC of 0.36 mm, and steel of 0.0095 mm. Based on the simulation the choice was down to silicon rubber, PDMS, and soft PVC as they allow a bigger displacement to occur. PDMS is not readily available in the form of an elastic tube. It would need to be cured and processed before being a viable option. This in turn means that the choice is down to soft PVC and silicon rubber. The decision was made to use an inflatable pouch made of soft poly-vinyl chloride material.

Table 4

COMSOL Simulation results using 2-D axisymmetric object

	Material	Pressure (Pa)	Physics/Study	L(mm)	Inner D (mm)	Outer D (mm)	Deflection δ (mm)
2-D	PMMA and air	10665.78	Laminar flow/stationary	420	174.2	180	0.0043
2-D	PDMS and air	10665.78	Laminar flow/stationary	420	174.2	180	15.6
2-D	Silicone rubber and air	10665.78	Laminar flow/stationary	420	174.2	180	0.23
2-D	Soft PVC and air	10665.78	Laminar flow /stationary	420	174.2	180	0.36
2-D	Steel AISI 4340	1200000	Laminar flow/stationary	609.6	125	130	0.0095

3.3.3. **Analysis and Discussion**. The percentage difference can be calculate using the equation:

$$\left|\frac{experimental\ - theoratical}{theoratical}\right| \times 100$$

Where the theoretical value is the calculated result based on thin walled theory, and the experimental value is the COMSOL result based on having to choose the different parameters. There is an inconsistency between the COMSOL and calculated results.

With a long thin walled cylinder with a small diameter, and shorter with small diameter, a difference in the meridional bulge is expected with respect to the length over the diameter, all else equal, and is not predicted by thin walled cylinder theory. The longer cylinder will show a bigger displacement profile than a shorter cylinder. The ends of the cylinder are held against radial growth but are permitted to translate laterally. Closed-form solutions are obtained on the assumption that the bulged meridional profile can be represented by successively larger circular sections at increasing pressures [55]. In the calculated results, the length of the cylinder structure makes a big difference and is not represented in the equation for thin walled cylinder theory. However, in the simulation the length is an important aspect and affects the general displacement of the cylindrical tube.

This can be used to explain why the huge error between the COMSOL simulations results and the calculated results found on Table 5. Another aspect is that COMSOL uses the Navier-Stokes equation, and is represented by a completely different equation. The displacement of the COMSOL simulation were affected by components such as structural mechanics, laminar flow, and meshing. Since each method used different equations and parameters, a difference is to be expected.

Table 5

Comparison of calculated vs COMSOL results

Material	Calculated results (mm)	COMSOL results (mm)	Error %
PMMA	0.0043	0.015	252.50
PDMS	59.58	15.6	73.81
Silicone Rubber	1.75	0.23	86.85
Soft PVC	1.27	0.36	71.65
Steel AISI 4340	0.0040	0.0095	190.86

Figure 7 represents the meshing and geometry of the simulation done for the soft PVC material. The length of the tube is 420 mm long and characterizes the length of a pregnant uterus. In a 2-D asymmetric simulation, the cylindrical tube may be represented as simple shapes such as rectangles. There are 2 rectangles, one with a width of 174.2 mm and the outer width which is180 mm. This creates a thickness of 5.8 mm representing the thickness of the uterus. Figure 7 also provides a closer look of the style of meshing done to compute the displacement. The choices of meshing for a 2-D axisymmetric object are boundary layer, free triangular, free quad, mapped and their combinations. Each of these meshing options has different geometry and computes the displacement based on set geometry.

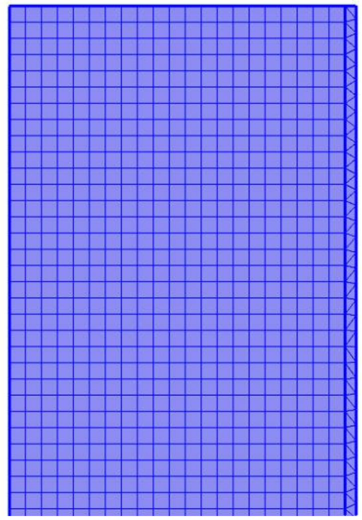

Figure 7. Mesh profile of soft PVC tube.

When the physics based meshing option was done, it resulted in a displacement of 0.36 mm. Table 6 represents some of the mesh types and the information found after the simulation. The information includes iteration number, number of elements, run time, and error at final time step. After doing the boundary layer, free triangular, free quad, mapped, and the combination of mapped and boundary layer, the results were 0.35 mm, 0.34mm, 0.35 mm, 0.36 mm, and 0.36mm respectively. After comparing each user defined mesh with the physics-based mesh, the mapped and mapped plus boundary layer meshing option had the same displacement as the physics based meshing. This could indicate that the physics-based mesh found that a mapped topology was the ideal option. The combination of mapped and boundary layer was the ideal meshing option because it considers the geometry of the shape as well as its boundary. Therefore, the number of elements increase from 7672 for the mapped to 7904 for the mapped and boundary layer. The run time conversely increased to account for the increase of elements. The time step for both the mapped and the mapped and boundary layer were the same as well as the error at the final time step.

Table 6

Comparison between 5 mesh settings

Mesh type	Mesh information		
	Time step	Number of elements	Run time (s)
Boundary layer	10	3435	3
Free triangular	10	3435	3
Free quad	10	3806	3
Mapped	11	7672	4
Mapped + boundary layer	11	7904	5

Figure 8 illustrates the displacement on the tube after all the parameters and meshing has been completed. The total displacement of the soft PVC tube was computed to be 0.36 mm. From figure 8, most of the displacement occurs in the middle of the object and none occur at ends. During the simulation, a capped wall anchor was place at each end of the soft PVC inflatable tube. The anchor are placed there to show that the pressure is contained within the structure.

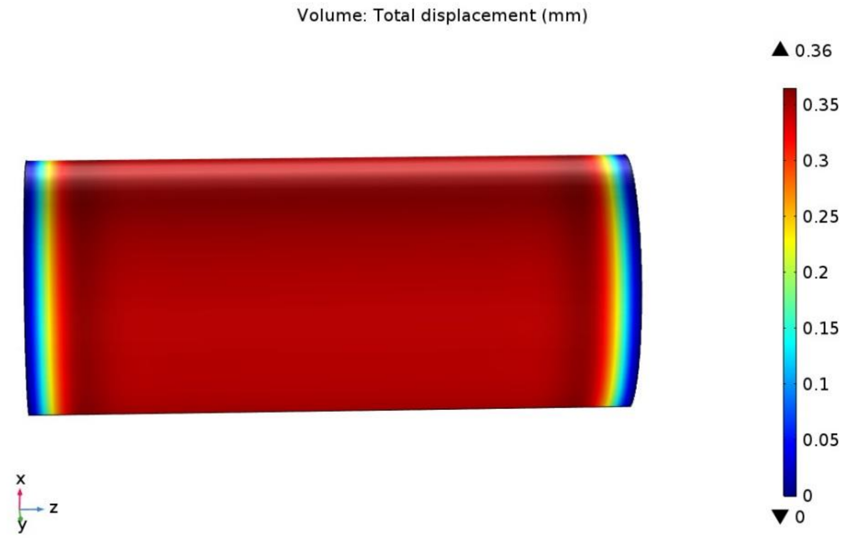

Figure 8.Displacement of soft PVC tube.

Prior to creating a device to exhibit the mechanical activity of the uterus some preliminary steps were taken. One such step was to calculate the displacement using the equation for thin-walled cylindrical theory. Four calculations were done to choose which material would be best for creating the device, which are PDMS, PMMA, silicon rubber and soft PVC. Based on the calculation and the COMSOL simulation, soft PVC was chosen as the material of choice due to having the least deviation from the other materials. To create a device exhibiting the uterine contraction signal an inflatable tube made of soft PVC was selected. This calculated and COMSOL simulation confirms that uterine like contractions can be achieved using soft PVC. A displacement of 1 mm during a uterine contraction is a reasonable assumption to make.

3.4. Inflatable Pouch

3.4.1. Experimental Setup. After the simulation and the cylindrical tubular calculation, the device exhibiting uterine-like contractions was developed. The device was made using an inflatable pouch of soft PVC. To give the inflatable pouch a sturdy shape, a cylindrical ofbject of smaller diameter was inserted into the inflatable pouch. The device used to pressurize the inflatable tube is a KNF micro-diaphragm gas-sampling pump powered by an Arduino power supply Also involved is a TOCO which provides a pressure sensor that measures the internal pressure rise when the uterus contracts. This method of exhibiting the uterine contraction signal is a proof of concept and will be further improved. Using the TOCO, two things could be determined, the duration of the contraction as well as the relative intensity of the uterine contraction. These were the two parameters used to test the inflatable pouch. The inflatable tube will be attached to the air pump tube via a hose. The TOCO gauge sensor is wrapped around the inflatable tube and capture the relative intensity produced by the air pump.

3.4.2. Procedure. Three rounds of testing were conducted representing the different stages of labor during pregnancy found on Table 7. They are the early labor phase, active labor phase, transition phase. The contraction time, relaxation time, and the reading of the TOCO are the parameters observed during the tests. The contraction time is the amount of time it took for the pouch to inflate and the TOCO to measure the internal pressure. This starts at whatever baseline the TOCO picks up before the air pump starts to run. The next part is the relaxation time, which is the amount of time it took for the air to come out of the inflatable pouch. The relaxation time was recorded as soon as the inflatable pouch went down to its baseline limit. Another parameter was the pressure recorded by the TOCO of the inflatable pouch when air was being pumped through it.

Table 7

Information on contraction length, frequency and strength during labor [56]

	Contraction length	Contraction frequency	Contraction strength	What women feel during contractions
Stage 1: Early labor phase	30 – 45 seconds	5 – 30 min apart, may be irregular	Begins mild and becomes stronger	back pain, menstrual cramps, and/or pressure in pelvis
Stage 2: Active labor phase	45 - 60 seconds	3 - 5 min apart	Stronger than the first stage	Stronger, longer, and more intense than early labor
Stage 3: Transition phase	60 - 90 seconds	30 seconds - 2 min apart	Very strong and intense	Highly intense, experiences chills, nausea/vomiting

3.4.3. Results and Discussion. The first series of tests uses the contraction length of 37.5 seconds to represent the early labor phase. The early labor phase is the time of onset of labor. The second series of test uses the contraction length of 60 seconds to represent the active labor stage. The third series of data, a contraction time of 90 seconds represents the transition stage. They are the basis of the the test conducted on Table 8. Table 8 represents the testing of the inflatable pouch using the contraction length, where C is the contraction time in seconds, R is the relaxation time in seconds, and TR is the TOCO reading. These tests are done to show that the pouch is able to actuate a similar bio-physiological signal response as the uterus.

Table 8

Testing of the inflatable pouch using contraction length

	Round 1			Round 2			Round 3		
	C (s)	R (s)	TR	C (s)	R (s)	TR	C (s)	R (s)	TR
Test 1	37.5	~ 6.5	285	60	~ 9.3	285	90	~ 8.2	282
Test 2	37.5	~ 6.2	283	60	~ 7	280	90	~ 9.1	283
Test 3	37.5	~ 6.8	282	60	~ 6	283	90	~ 8.5	285
Test 4	37.5	~ 5.4	280	60	~ 6.5	279	90	~ 8.4	287
Test 5	37.5	~ 6.9	284	60	~ 7.3	285	90	~ 10	286
Test 6	37.5	~ 7.6	279	60	~ 8.3	288	90	~ 7.6	285
Test 7	37.5	~ 5.5	285	60	~ 8.7	289	90	~ 8.9	289
Test 8	37.5	~ 6.7	280	60	~ 6.6	287	90	~ 9.2	285

A TOCO usually uses a spring-loaded pressure sensor that detects uterine contractions. The external monitor does not read in any particular unit and is not measured quantitatively. When starting the test, one reoccurring theme was the baseline of the TOCO changing when the pressure sensor was attached to the inflatable pouch. Since the baseline changes every test, the best way to assure that the test is accurate was to make sure that the contraction time starts at the baseline and that the relaxation time ends at the same baseline. During the duration of this experiment, two inflatable pouches were used. Before testing, a preliminary study was conducted on the inflatable pouch to test its capability. The first pouch ended up tearing and became unusable.

Since the first pouch broke, a second pouch was used to continue the experiment. The first round of testing conducted for 37.5 seconds, had TOCO readings of 285, 283, 282, 280, 284, 279, 285, and 280. The second round of test was conducted with contraction time of 60 seconds, from test one through test eight the TOCO readings were 285, 280, 283, 275, 289, 288, 289, and 287. The third round of data, which had a contraction time of 90 seconds yielded results such as 282, 283, 285, 287, 286, 285, 289 and 285. The importance of these numbers is that they exemplify the relative intensity of a contraction during gestation. A typical reading of a contraction using a tocodynamometer ranges from 80 – 240+ depending on many factors. This is reassuring because we have been able to produce a device containing similar bio-physiological readings of a contraction during labor.

Figure 9(a) represents the inflatable pouch in the relaxation phase. When the pouch is relaxed it will be at the baseline rate which is the minimum starting point used for comparison. This relaxation phase occurs after the contractional phase of the uterine contraction in the female body. After placing the external TOCO , one should record the baseline level when there are no contractions occuring, otherwise the reading may be faulty. In Fig 9(a) for instance, the baseline rate was 14. Fig 9(b) represents the pouch when it is under contraction. The reading from the TOCO when the inflatabe tube is fully inflated is 216. In any case the contraction recorded from the TOCO of the inflatable tube is similar to that of a woman during pregnancy. A true contraction during labor can reach number as high as 250 as indicated by Fig. 9(b).

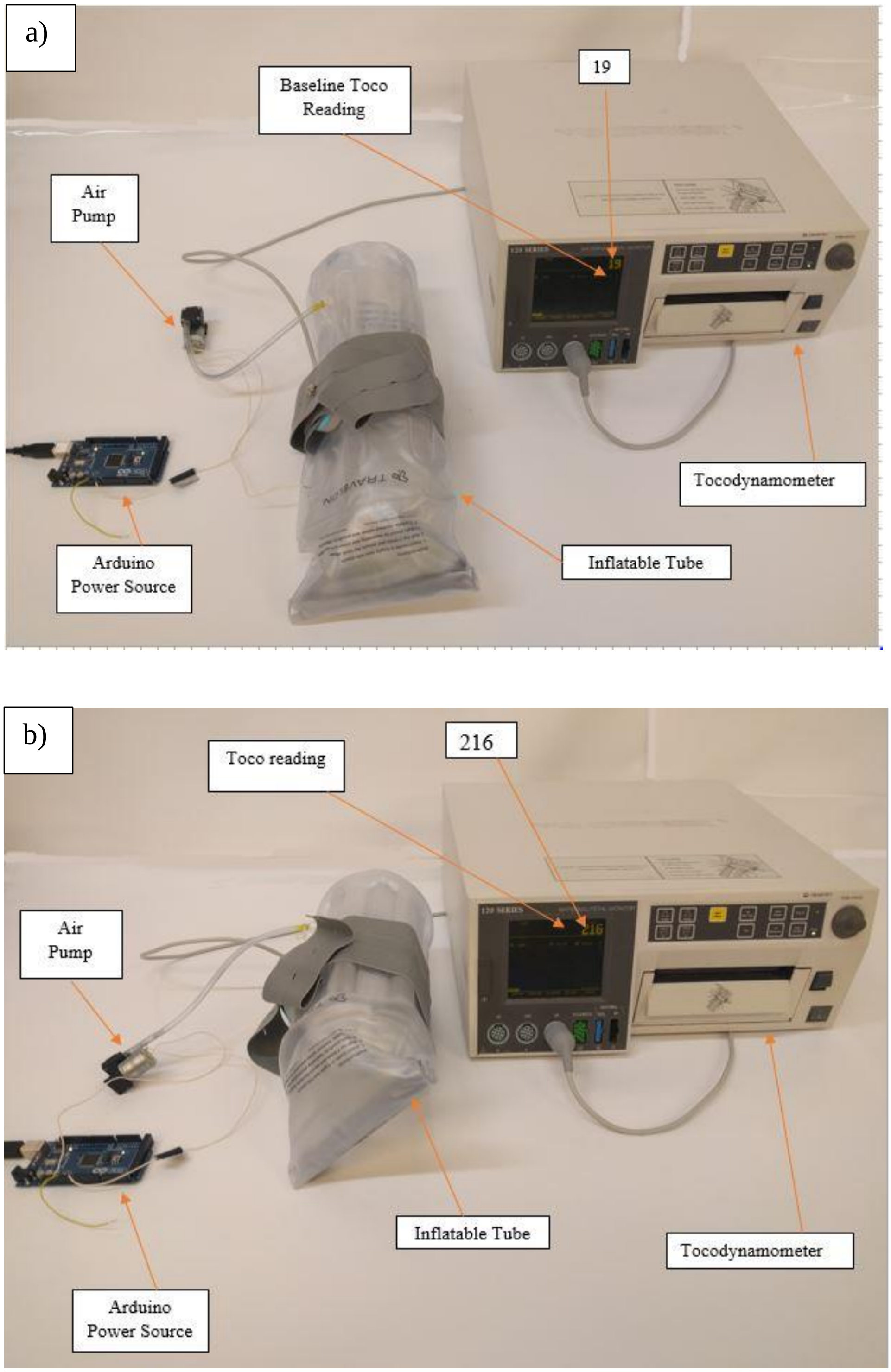

Figure 9. Setup of inflatable tube experiment. 9(a) is Baseline reading, 9 (b) is inflated reading.

3.5. Conclusion

The device used to represent the mechanical activity of the uterus has been created. This was done by calculating and simulating the displacement of elastic material to find the material best suited for simulating the uterine contraction. It involves an inflatable pouch made of soft PVC, an air pump motor and a power source for the motor in the shape of an Arduino. To imitate the mechanical activity of the uterus the motor was attached to the tube using a hose allowing air to flow through the inflatable tube. The device used to measure the mechanical activity of the uterus is the TOCO. The Parameters chosen for the testing of this device are contraction times, relaxation time and the reading of the TOCO. Therefore, three rounds of test were conducted around the different stages of labor. In test 1 the contraction was timed at 37.5 seconds to represent the early labor phase, test two was for the active labor phase timed at 60 seconds, and test 3 was the transition phase timed at 90 seconds. Each test was repeated for 8 times. During gestation, the contraction length changes which is why in each of the tests the contraction length was different. The TOCO was able to reach its maximum, which is at a reading of 289. To put all of this into perspective, a true contraction, experienced by a pregnant mother can go as high as 240+ when measured by a TOCO.

Chapter 4

Design of Electrical Signal of the Fetal Heart Using LabVIEW and Data Acquisition Device

4.1. Introduction

Fetal ECG is an important way to assess the health of a fetus. The purpose of this chapter is to create a device that exhibits all bio-physiological signals both normal and abnormal. The idea behind this chapter is using LabVIEW and DAQs to produce the electrical activity of the fetal heart. One of the more common complications occurring to a fetus during pregnancy is fetal hypoxia. Fetal hypoxia occurs when the fetus is deprived of oxygen. Fetal hypoxia may occur from a number of reasons, umbilical cord prolapses, cord occlusion, placental infarction, and maternal smoking. Fetal hypoxia is one the root causes of abnormal ECG signals in fetal development. Another issue that should be exhibited by the device is the abnormal signals caused by congenital heart disease (CHD). CHD is the most common severe congenital irregularity worldwide. The incidence of CHD is estimated at 6-12 cases per 1000 live births[57].

Continuous fetal heart rate (FHR) monitoring is a routine for obtaining significant information about the fetal condition during labor. The intrapartum fetal ECG (fECG) has been shown capable of detecting newborn acidemia, and other cardiac anomalies. It is generally known as the noninvasive FECG, which can monitor the FHR through the maternal ECG by placing electrodes on the mother’s abdomen, and many researchers have developed signal processing methods to derive the FECG from the ECG recorded from the mother [58]. Therefore, there is a need to create normal and abnormal ECG signals since every birth may be different.

4.2. Fetal Heart Rate

The heart is the organ responsible for pumping blood throughout the body and is the center of the circulatory system. This system comprises of a system of blood vessels, such as arteries, veins and capillaries. An electrical system controls your heart and uses electrical signals to contract the heart's walls. Figure 10 displays the different components of the electrical activity of the heart. When the walls contract, blood is pumped into the circulatory system. Inlet and outlet valves in the heart chambers ensure that blood flows in the right direction [59]. The wall of heart consists of three layers of tissue called the endocardium, myocardium, and epicardium. The myocardium is where the electrical activity of the heart occurs.

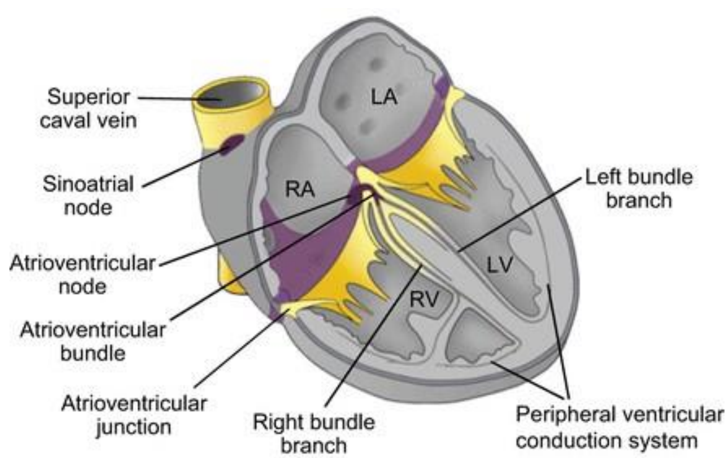

Figure 10. The components of the cardiac conduction system[60].

To grasp how the ECG functions, there is a need for understanding the basic physiology of the heart. The heart is made of four chambers, the left and right atrial and ventricular chambers. Each one of these chambers has an important role in the function of the heart. The right atrium receives deoxygenated blood from the body and pumps it into the right ventricle to send to the lungs to be oxygenated. The left atrium holds blood returning from the lungs and acts as a pump to transport blood to other areas of the heart. The left ventricular chamber is responsible for pumping oxygenated blood to tissues all over the body [61].

The heart is known as a muscular pump whose activity provides the work necessary to drive blood around the body. To function proficiently as a pump a sequence of events must occur called the heart cycle. This sequence of events is controlled by the electrical properties of the cell [62]. After the initiation of the pacemaker cell, the electrical activity spreads thought the heart, reaching every cardiac cell rapidly with correct timing [63]. The heart muscle is made of tiny cells. The heart’s electrical system controls the timing of the heartbeat by sending an electrical signal through these cells. The two types of cells that permit the electrical signal to control the heartbeat are the muscle and conducting cells. The muscle cells enable the heart’s chambers to contract and the conducting cell that carry the heart’s electrical signal. The electrical signal travels through the network of conducting cell, which stimulates the atria and causes the ventricles to contract [64].

All action is coordinated by an imperative set of structures, the hearts electrical system. Contractions begin when an electrical signal goes to the individual heart muscle cells. The heart has a natural pacemaker that regulates the pace or rate of the heart known as the Sino-atrial (SA) node where the heartbeat starts. The sinus node sends the impulse that makes the top of your heart contract. The impulse then travels to the middle of the heart to the atrioventricular (AV) node, which sends a message to the ventricles to pump blood to the lungs and the body [65].

From the sinus node, the electrical impulse starts by spreading throughout the atria (from right to left). When this happens, the cells lose their internal negativity, a process known as depolarization. The depolarization of the atria causes them to contract. The electrical current then spreads to the AV node. In order to depolarize the ventricles, the electrical impulse travels through the bundle of His, along the right and left bundle branches, and ends at the Purkinje fibers. This process causes depolarization of the ventricles, causing them to contract. While the ventricles are being depolarized, the atria are regaining their internal electrical negativity, a process known as repolarization. [66].

At every beat, the heart is depolarized to trigger its contraction. The electrical activity is transmitted throughout the body and can be picked up on the skin. One of the safest ways to measure the electrical activity of the fetal heart is by using the electrocardiogram (ECG). ECG is a non-invasive method, which uses skin electrodes to record the biological signal of the human heart. Graphically. Similar to a standard electrocardiogram, which measures the wellbeing of a fully-grown human, the fetal/abdominal ECG is a sensitive indicator of the fetal health state. The electrode is a sensor consisting of a metal and often a salt bridge, which converts the local differences of the concentration of charged ions into electrical signal. The bioelectric signal measured from the surface of the skin is mostly in the range of 0-2 mV [67]. An ECG involves attaching 10 electrical cables to the body: one to each limb and six across the chest. The result of the ECG is illustrated in Figure 11.

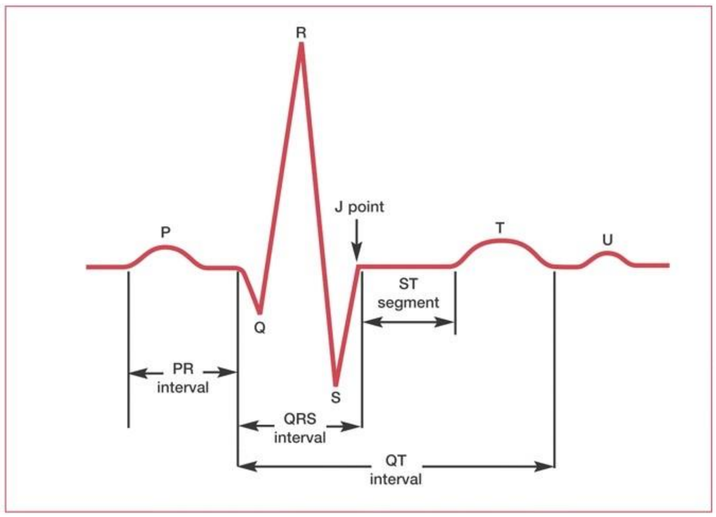

Figure 11. The basic pattern of electrical activity across the heart P, QRS, T profile [67].

The basic pattern of the ECG's electrical activity was discovered over one hundred years ago. It incorporates three waves, named the P, QRS (wave complex), and T waves. The P wave represents atrial repolarization. PR interval is the time between the first deflection of the P and the first deflection of the QRS complex. The QRS complex represents ventricular depolarization. The ST segment, which is also known as the ST interval, is the time between the end of the QRS complex and the start of the T wave. T waves represent ventricular repolarization, and atrial repolarization is concealed within the large QRS complex. When disturbances of the conduction system are present, this can be detected via abnormalities of the spikes and waves on an ECG[67].

Testing of the electrical activity of the heart can be conducted easily; therefore, many studies could be done on the electrical activity of the heart. One such test was conducted by James P Neilson who articulated that the repolarization of myocardial (heart muscle) cells is very sensitive to metabolic dysfunction and may be reflected in changes of the ST waveform. Thus, in adults with myocardial infarction or exercise-induced angina pectoris from coronary artery disease, the ST segment may be elevated [36]. This test involved using the basic ECG patterns to assess the health of a fetus as well as adults with heart disease.

One reoccurring situation in the signal acquisition of the fetal heart is the presence of noise. Karvounis et al articulates that the sources of interference when acquiring the abdominal signals are: the maternal ECG, myographic noises, powerline interference, the fluctuation of the baseline and factors related to the gestation week[68]. This makes it difficult to obtain significant readings of the fetal heart. This is one of the biggest problems encountered in the fetal electrocardiography interpretation. The electrode used to gather the bio-physiological signal of the heart could be a source of distortion as well. The cables between the electrode and the measurement system can also introduce the artifacts and noise.

Authors deal with signal processing in different ways. According to a review done by Sameni et al on the fetal ECG signal, the different signal processing and data analysis methods for the fetal heart rate are direct fetal ECG analysis, adaptive filtering, linear decomposition, nonlinear decomposition, forward modeling, and inverse solution. In early works fetal detection was done over raw data without any processing [69].

Table A2 in Appendix A displays a general comparison between existing methods of fetal ECG analysis. It describes the signal processing methods for single and multichannel systems. This is relevant since a multichannel signal of noise; maternal and fetal signal will be created. These methods consist of training an adaptive or matched filter for either removing the maternal ECG using one or several maternal reference channels, or directly training the filter for extracting the fetal QRS waves. Decomposition of single or multiple channel recordings is another common approach. In this method, the signals are decomposed into different components by using suitable basis functions. Linear decomposition methods using either fixed basis functions, or data-driven basis functions have limited performance for nonlinear and degenerate mixtures of signal and noise. [69].

4.3. Experimental Setup

Overall, the goal is to create a device exhibiting the electrical activity of the fetal and maternal heart. Creating the electrical activity requires a few components. This includes a LabVIEW program along with the DAQs. Some other components that ensure its creation is a conductive medium (foil), alligator clips, resistors, and electrodes. Another constituent is the maternal and fetal signal found using the LabVIEW program and the signal processing of the fetal ECG.

4.4. Procedure

To produce the electrical activity of the heart a few preliminary steps were taken. The first step was to use a function generator to produce a sine signal and use an oscilloscope to read the signal. The sine signal was transmitted through an aluminum foil medium. The function generator contains a built in ECG signals. Therefore, the ECG signals replaced the sine signal. The next step was to move away from the bulky devices such as the function generator and oscilloscope. The function generator, foil, electrodes, alligator clips, and the (DAQ) were used. The DAQ takes the place of the oscilloscope and receives the signal generated by the function generator on LabVIEW. The DAQ that receives and processes the ECG signal is the NI USB 6210 Data acquisition device with 16 inputs, has 16-bit resolution, and a process 250 KS/s from National instruments.

Subsequently, a device capable of generating the signal replaces the function generator. The device used to replace the function generator is another DAQ whose specific job is to generate a waveform. The DAQ used to generate the signal is the NI USB-4431 that has 24-bit resolution and can process 102.4 Ks/s from National Instruments. This DAQ has one output port, which allows the generated signal to reach the foil medium through a probe. This probe is connected to one side of the alligator clip and linked the end of the foil using the other side

An electrode is helps in the transmission of the signal from the foil to the receiving DAQ NI USB 6210. Foil is highly conductive material the current can flow freely throughout the whole medium. The first attempt was done using one foil medium as a proof of concept. After a successful test with one foil, the next step was to use multiple pieces of foil. An ECG signal when taken differs slightly in amplitude at each location based on their location during an exam. The software used to create the maternal and fetal ECG signals used to create the electrical activity of heart is LabVIEW.

When measuring the electrical signal of the heart using ECG electrodes, the signal will be different at each spot where the electrodes are found. Foil is highly conductive, and it has to be separated into a 4-array foil connected by resistors to create a change in the amplitude of each ECG signal. The type of resistor used was 39 kΩ resistors. The electrical signal of the fetal heart is measured from the maternal abdomen. The two types of signals that are of interest for the electrical part of the project is the maternal ECG ranging from 60 -100 bpm (1 - 1.67 Hz) and the fetal ECG signal ranging 120 - 180 bpm (2 - 3 Hz).

When an ECG device detects the electrical activity of the heart, noise from different sources may occur. The ECG collects all of the signals that occur within an individual's body, as well as all surrounding noise and noises from the machines and electrodes. Mainly two types of noises are present in the ECG. Noise with high frequency including the EMG noise, additive white Gaussian noise and power line interference. The noises contaminated in the ECG signal may lead to inaccurate interpretation. Therefore, filters are required to oppose the noise. The types of filters used to get rid of noises are low pass and bandpass filter.

The band-pass filter is a filter that allows a certain band or spread of frequencies to pass through. The reason for the band-pass filter is that there are two different signal that have 2 different frequencies. The maternal ECG signal has a band-pass filter with low cutoff frequency of 0.1Hz and high cutoff frequency of 1.5 Hz. The fetal signal has a bandpass filter with a low cutoff frequency of 1.7 Hz and a high cutoff frequency of 2.5 Hz. This ensure that only frequencies from the desired range are present in the graph.

4.5. Results and Discussion

Both the maternal and the fetal signals were created using the biomedical toolkit found as an extension of the LabVIEW program. Figure 12(a) above represents the electrocardiogram of an adult person. Normally, the ECG ranges 1 Hz to 1.67 Hz where 2 peaks occur every second. The representative frequency used for the maternal signal is 1 Hz. The Amplitude of the maternal fetus is higher than that of the fetus meaning that the signal is stronger. Figure 12(b) represents the electrocardiogram of a fetus. The fetal electrocardiogram ranges from 2 Hz to 3 Hz. In this instance, 2Hz was chosen as the representation of the fetal electrocardiogram signal. The frequency of fetal heart beats faster but the amplitude is smaller. A fetus has smaller heart and therefore the heart needs to beat faster in order to pump the proper amount of blood. The maternal ECG overshadows the fetal signal, which incited the need to process the fetal signal in the mist of all other signals.

a)

b)

c)

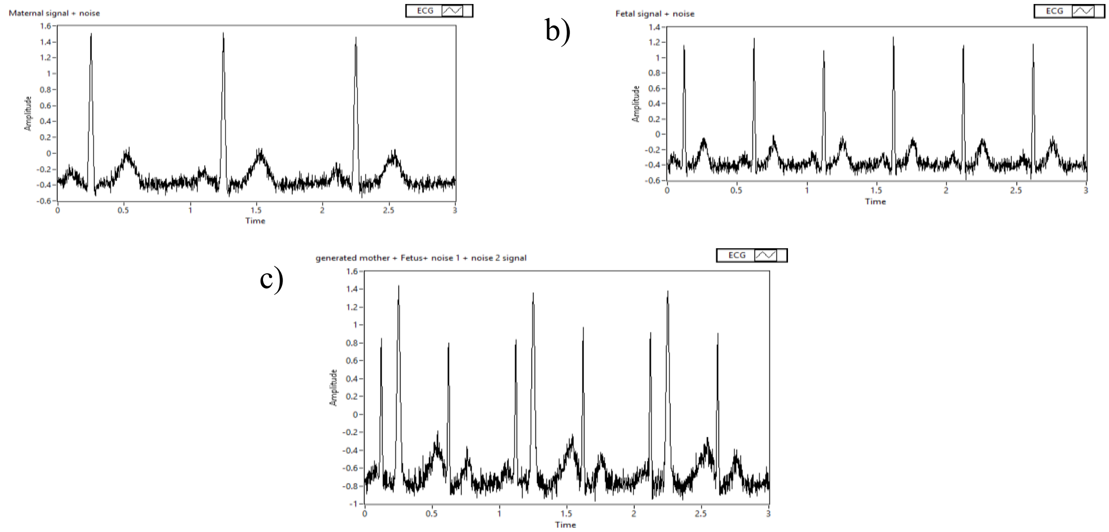

Figure 12. (a) Maternal ECG signal, (b) Fetal ECG signal, and (c) mixed fetal and maternal ECG signal.

Figure 12(c) above shows the combined signal of the mother and fetus. When the fetal ECG is conducted, all of the noises and signals will be mixed together. It is then, that signal processing can occur. Signal processing separate all of the signals and provide the fetal ECG.

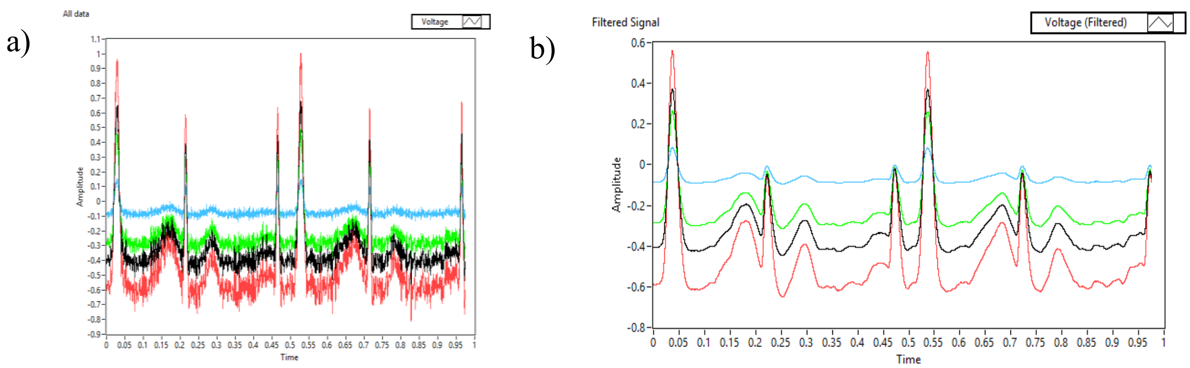

Figure 13. (a) Voltage change of mixed fetal and Maternal ECG (b) Filtered fetal and maternal mixed signal.

When taking an abdominal ECG, the signal will have a slight variation in voltage. The way to represent this is by splitting the maternal and fetal ECG into different amplitudes, as represented in Figure 13(a). The maternal ECG amplitude is approximately 1.5 mV for the mother and 1 mV for the fetus in the presence of noise. However, when filtered the approximate amplitude of the signal is 1 mV for the mother and 0.6 mV for the fetus. The red signal is the original and each subsequent signal represents a weaker signal. From the filtered signal, the signal starts at -0.6 mV and ends at 0.6 mV, which when counted will be 1 mV in amplitude. The same behavior occurs with the fetal signal, where the signal begins at 0 mV and ends at 0.6 mV which is counted as 0.6 mV in amplitude. This same behavior occurs with the other 3 signals, where the black signal is –0.4 mV to 0.4 mV for the mother and 0 to 0.4 mV for the fetus. The green of -0.3mV to 0.3mV for mother and 0 mV to 0.3 mV for the fetus. Lastly the blue -0.1mV to 0.1 mV for the mother and 0 mV to 0.1mV for the fetus.

To make the signal different at every spot some resistor to change the amplitude. Therefore, according to ohms law, if the voltage increases, the current will increase provided the resistance of the circuit does not change. To procure a drop-in amplitude, five 39 kΩ resistors were used and arranged in series. In a series circuit, the current through each component is the same, and the voltage across the circuit is the sum of the voltages across each component. When using the same resistance there is an even distribution between each of the signal.

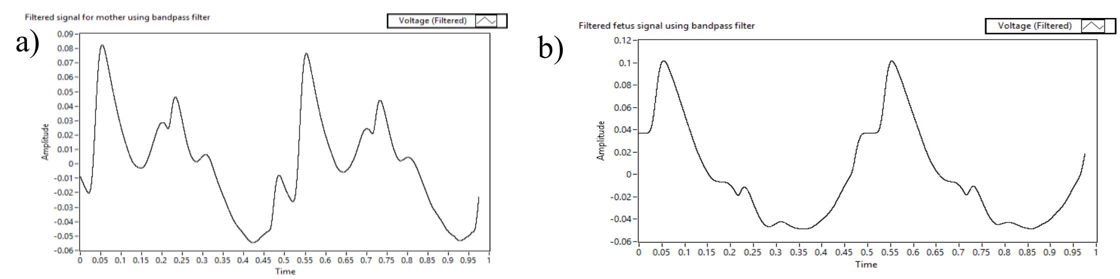

Figure 14. (a) Signal processing done for maternal signal (b) Fetal processing done for fetal signal.

Figure 14 represents the signal processing done using LabVIEW. This was done to split the signal back into the maternal and fetal signals and acquire the fetal signal. Maternal signal and fetal signal are 1 and 2 Hz signals. Since the signals are very close in frequency, it requires a complex signal processing method for filtering the fetal ECG signal. It would be easier to filter a signal with a greater difference of frequency in between them. Figure 14(a) represents the signal processing done for the maternal signal and, Figure 14(b) represents the signal processing done for the fetus. To split the maternal and fetal signals, a bandpass filter with low cutoff frequency of 0.1 Hz and a high cutoff frequency of 1.5 Hz was used, the topology used was a Butterworth filter of degree 1 for the mother. For the fetal signal a bandpass filter with a low cutoff frequency of 1.7 Hz and high cutoff frequency of 2.5Hz was used, the topology used was also a Butterworth filter of degree 1. From observing the signals, the ECG signal was not filtered properly. The maternal and fetal signal should resemble the same shape that was simulated.

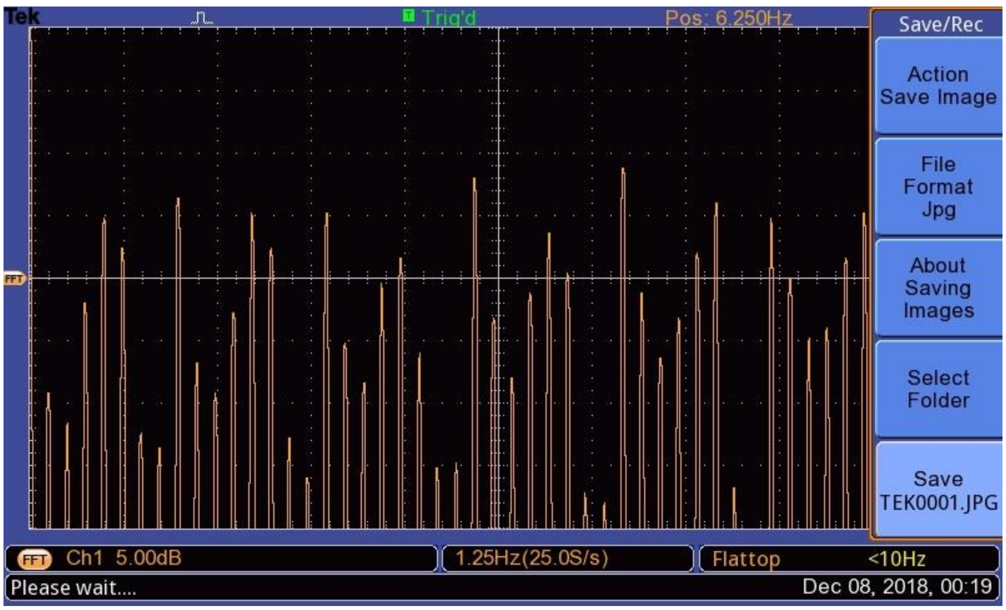

Figure 15. Fast Fourier transform of mixed maternal and fetal ECG.

Figure 15 shows the frequency domain representation of the mixed maternal and fetal ECG signals done using a Tektronix oscilloscope. According to Fourier series, the ECG signal is a mixture of sine signals of different frequencies, with peaks of different heights. A Fourier series receives the ECG signal and expresses it in terms of frequencies of the waves that make up the signal. This Fourier representation of the mixed ECG signal was done to make a filter for the known frequencies for signal processing. However, this will prove to be very complex due to the nature of the peaks.

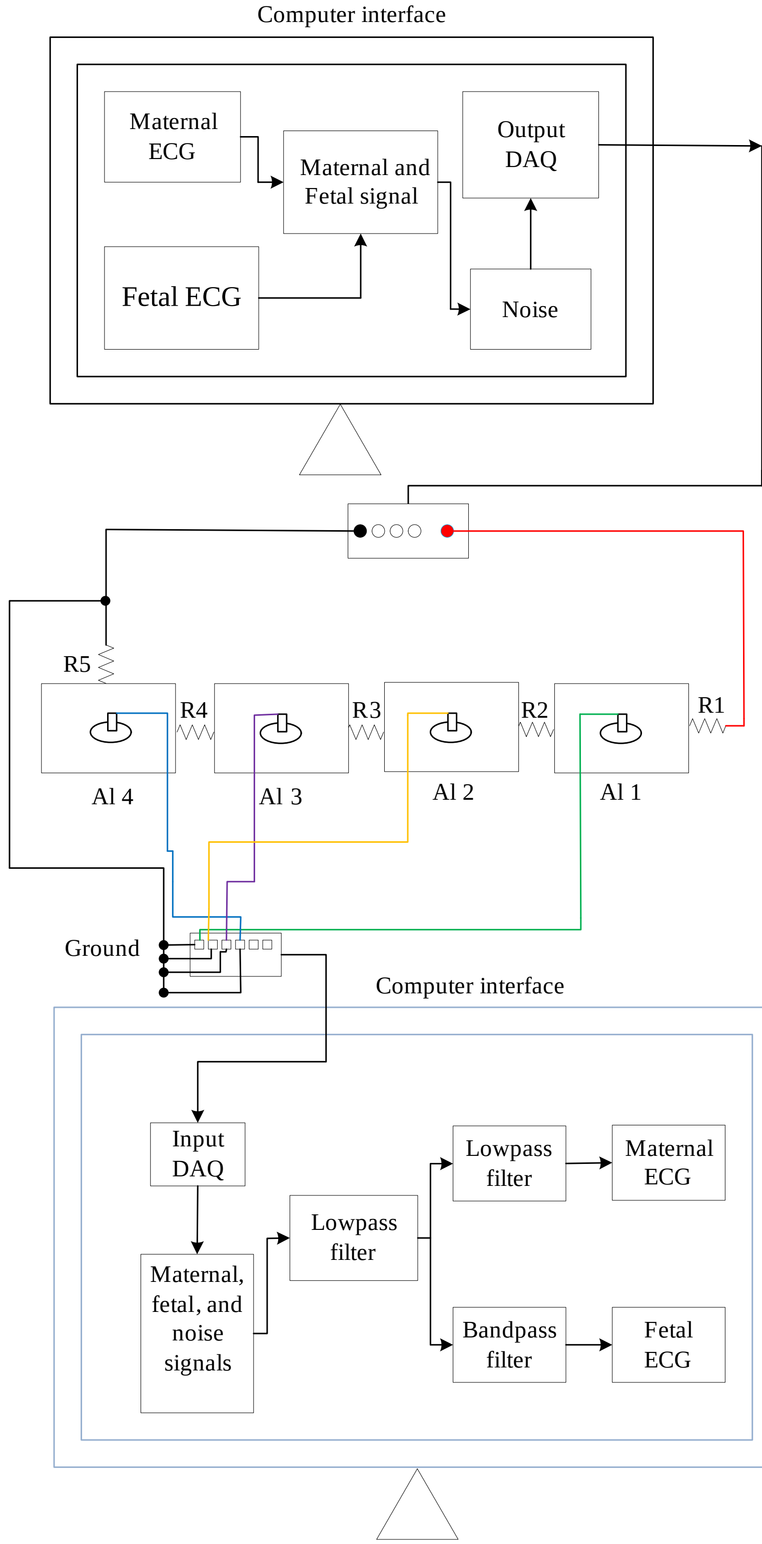

Figure 16. Electrical system architecture.

Figure 16 illustrates the process taken to generate the maternal and fetal signal, as well as how to read the received signal. Within the interface, a simulated maternal and fetal signal was generated and mixed with noise. From there the generating DAQ outputs the signal through each of the foils. The resistance chosen for this is a uniform resistance of 39 kΩ founded in between each foil to ensure amplitude drop. The red wire leaving the red circle represents the generating DAQ providing the signal all of the foils. It first goes through resistor, which produces the first potential drop. All of the subsequent wires are connected to each individual aluminum surface and are connected to the receiving DAQ. There are 4 wires because each signal will be slightly different. The green wire branching from Al 1 receives drop from R1, Al2 from R1 + R2, Al 3 from R1 + R2 + R3, and Al 4 from R1 + R2 + R3 + R4. R5 is the last resistor where black wires are connected and represents the ground for all of the foils. The receiving DAQ then inputs the signal back into the LabVIEW interface as a mixed fetal, maternal and noise signal for signal processing. This was done provide a basic diagram of what is going on in the picture below and the different components and how they are connected to one another.

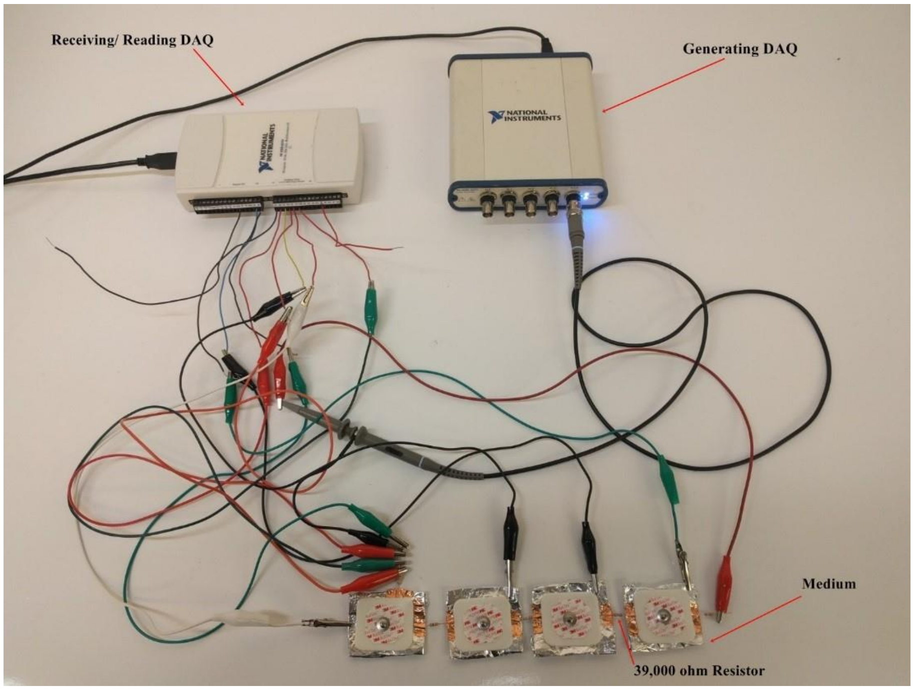

Figure 17. Experimental setup of electrical activity of fetal heart.

Figure 17 is a physical representation of how to produce the bio-physiological nature of the fetal heart. The DAQ to the right is used to generate the signal the mother and fetus and the DAQ to the lefts receives the signals in preparation of the signal processing to get the fetal heart signal.

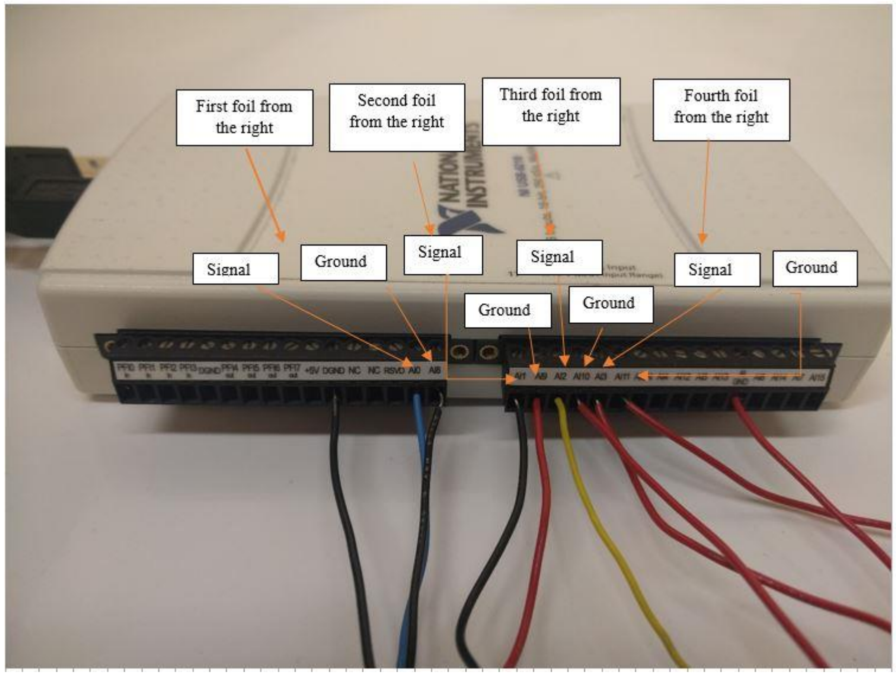

Figure 18. Data Acquisition of Signals.

Figure 18 describes how the Data Acquisition device reads each individual signal. Each foil has a signal that corresponds to it. The first foil from the right corresponds to A|0 and A|8, where A|0 is where the received signal read by the DAQ and A|8 is the ground. All other signals take the same format. Each port has a ground to protect the DAQ from any surges of electricity. Therefore, each port needs one. There are 4 ports used for the four different signals. The second foil from the right is devised of the signal and ground categorized by A|1 and A|9. The third foil is labeled by A|2 with a ground of A|10. Lastly, A|3 and the ground A|11 characterize the fourth foil from the right. Overall, these combinations signal ports and ground is what helps the creation of the ECG signal of the fetus and the mother.

4.6. Conclusion

The goal was to create a device that exhibit the fetal heart rated signal. During a fetal signal, the fetal signal is mixed in with the maternal signal and different sources of noise. Therefore, creating a signal that exhibits all of these different components is important. Figures 12(a) and 12(b) represent the maternal and fetal signal with noise mixed in. Figure 12(c) displays the type of signals pick up by the fetal ECG machines while trying to get the fetal signal. The fetal ECG uses 10 lead electrodes to measure the fetal heart rate at different locations on the pregnant woman's body. Therefore, the signal will be different at each electrode location. This represents the drop-in amplitude of the single as seen in Figure 13(a). Since the ECG uses 10 lead electrodes, essentially the Figure 13(a) should essentially be 10 different signals. As a proof of concept, 4 signals were used instead. To procure a drop-in voltage, resistors were used. The amplitude is measured as a voltage and from Ohm's' law, voltage is inversely proportional to resistance. Additionally, signal processing on the mixed signal was done to separate the maternal and fetal signals. However, the attempt at processing the fetal signal was a failure. Figure 14(a) and 14(b) do not resemble the ECG signal from figure12 (a), and Figure 12 (b).

Chapter 5

Conclusion, Limitation, Future Works

5.1. Conclusion

The goal was to create a device that exhibit the mechanical activity of the uterus and the electrical activity of the heart. The first attempt at creating the mechanical activity of the uterus was with the use of muscle wire. Unfortunately, the muscle wire did not give the needed mechanical signal. Second attempt was done using an inflatable wine pouch to produce the mechanical activity of the uterus. Prior to using the inflatable tube to produce the mechanical activity of the uterus, hand calculation and COMSOL calculation were used to find the displacement and to ensure the right material is chosen. The testing of the device yielded a maximum value of 289. The last part was to create a device that can exhibit the electrical activity. This was done using Data acquisition devices and the LabVIEW program. The maternal and fetal signal were simulated, and the heart rate were 60 bpm and 120 bpm, which are 1Hz and 2 Hz in the frequency domain. After signal processing was performed to separate the maternal and fetal signals, it did not return the same shape as the simulated maternal signal. The filters altered the frequency and shape of the maternal and fetal signals. Overall, the goal of creating the electromechanical device was a success. This is the first prototype and has a lot of room for improvement before becoming a commercially viable product.

5.2. Future Works

Each of the methods conducted to create an electro-mechanical device exhibiting the mechanical signal of the uterus and the electrical activity of the heart has limitations. The limitation of the muscle wire was the amount of wires and power needed to actuate the mechanical activity of the uterus. The inflatable pouch also has its limitation such as that it is not a perfect cylinder. As seen from fig. 11A the pouch has air pocket to protect the bottle. These grooves can be a source of limitation since it will press unevenly against the pressure gauge of the TOCO. Explore other simulation software such as ABACUS and ANSYS for materials that have large deformation to obtain a more accurate answer of the displacement. Lastly, another limitation is in the electrical activity of the fetal heart. The first limitation is the aluminum foil is very conductive. Perhaps a less conductive material would be best. The next limitation is in the signal processing of the fetal and maternal ECG. Signal processing for the maternal and fetal ECG signals was quite hard to separate.

Finding a more realistic biocompatible material to represent the structure is of importance. A material that will allow for the transmission of signals from the body to the devices used to measure the bio-physiological signals. This material should also share similar dimension and structure as the uterus during labor. On a related note, adding a device to the structure that will allow the air pump to be automated. During testing, the air pump was connected and disconnected manually. One way to have the mechanical pouch inflate and deflate may be to use a programmable Arduino device. The motor should be programmable and be able to function with the use of a computer program such as c++, python, MATLAB. Another area where this device could improve is in the signal processing of the maternal and fetal ECG signal. For example, making different filters for signals of an ECG. Resistors/thermistors exist that allows current or other sources of heat to change the amplitude of a signal. Net step is to replace the DAQ with a smaller device, which could exhibit the same electrical signals as the fetal heart

References

[1] Z. Alfirevic, D. Devane, and G. M. L. Gyte, "Continuous cardiotocography (CTG) as a form of electronic fetal monitoring (EFM) for fetal assessment during labour," *Cochrane Database of Systematic Reviews,* vol. 5, no. 5, p. CD006066, 2013.

[2] M. P. Nageotte, "Fetal heart rate monitoring," *Seminars in Fetal and Neonatal Medicine,* vol. 20, no. 3, pp. 144-148, 2015.

[3] M. J. Stout and A. G. Cahill, "Electronic Fetal Monitoring: Past, Present, and Future," *Clinics in Perinatology,* vol. 38, no. 1, pp. 127-142, 2011.

[4] W. R. Cohen, "Clinical assessment of uterine contractions," *International Journal of Gynecology & Obstetrics,* vol. 139, no. 2, pp. 137-142, 2017.

[5] D. Ayres-de-Campos and Z. Nogueira-Reis, "Technical characteristics of current cardiotocographic monitors," *Best Practice & Research Clinical Obstetrics & Gynaecology,* vol. 30, pp. 22-32, 2016.

[6] (2019, 2/26). *Meet The Worlds most lifelike Childbirth Simulator Victoria*. Available: https://www.gaumard.com/s2200-victoria-childbirth-simulator

[7] V. Chudáček *et al.*, "Open access intrapartum CTG database," *BMC pregnancy and childbirth,* vol. 14, no. 1, p. 16, 2014.

[8] (2014). *Koala Toco Electronics-Free Tocodynamometer for Tracking Uterine Contractions*. Available: https://www.medgadget.com/2014/10/koala-toco-electronics-free-tocodynamometer-for-tracking-uterine-contractions.html

[9] K. Bhogal, "Focus on cardiotocography: Intrapartum monitoring of uterine contractions," *British Journal of Midwifery,* vol. 25, no. 8, pp. 491-497, 2017.

[10] C. N. Smyth, "*The Guard-Ring Tocodynamometer : Absolute measurement of Intra-Amniotic Pressure by an Instrument*," *BJOG: An International Journal of Obstetrics & Gynaecology,* vol. 64, no. 1, pp. 59-66, 1957.

[11] H. Eswaran, J. D. Wilson, P. Murphy, E. R. Siegel, and C. L. Lowery, "Comparing the performance of a new disposable pneumatic tocodynamometer with a standard tocodynamometer," in *Acta Obstetricia et Gynecologica Scandinavica* vol. 95, ed. Hoboken Wiley-Blackwell, 2016, pp. 319-328.

[12] U. M. P. INC, " *Intran® Plus Intrauterine Pressure Catheters*," ed. Utah Medical, 2017.

[13] E. Hadar, T. Biron-Shental, O. Gavish, O. Raban, and Y. Yogev, "A comparison between electrical uterine monitor, tocodynamometer and intra uterine pressure catheter for uterine activity in labor," *Journal of Maternal-fetal & Neonatal Medicine,* vol. 28, no. 12, pp. 1367-1374, 2015.

[14] P. J. Steer, M. C. Carter, A. J. Gordon, and R. W. Beard, "*The Use of Catheter-Tip Pressure Transducers For The Measurement of Intrauterine Pressure In Labour*," *BJOG: An International Journal of Obstetrics & Gynaecology,* vol. 85, no. 8, pp. 561-566, 1978.

[15] J. J. H. Bakker, P. F. Janssen, B. W. J. Mol, D. Papatsonis, J. M. M. Van Lith, and J. A. M. Van Der Post, "Use of intra-uterine pressure catheter (IUPC) versus external tocodynamometry (TOCO) during labour for reducing adverse outcomes," *Cochrane Database of Systematic Reviews*, no. 1, 2008.

[16] C. Muszynski, T. Happillon, K. Azudin, J.-B. Tylcz, D. Istrate, and C. Marque, "Automated electrohysterographic detection of uterine contractions for monitoring of pregnancy: feasibility and prospects," *BMC Pregnancy and Childbirth,* journal article vol. 18, no. 1, p. 136, May 08 2018.

[17] P. S. La Rosa, A. Nehorai, H. Eswaran, C. Lowery, and H. Preissl, "Detection of uterine MMG contractions using a multiple change-point estimator and K-means cluster algorithm," *International Congress Series,* vol. 1300, pp. 745-748, 2007.

[18] A. Furdea, H. Eswaran, J. D. Wilson, H. Preissl, C. L. Lowery, and R. B. Govindan, "Magnetomyographic recording and identification of uterine contractions using Hilbert-wavelet transforms," *Physiological Measurement,* vol. 30, no. 10, pp. 1051-1060, 2009.

[19] H. Eswaran, H. Preissl, J. D. Wilson, P. Murphy, S. E. Robinson, and C. L. Lowery, "First magnetomyographic recordings of uterine activity with spatial-temporal information with a 151-channel sensor array," *American Journal of Obstetrics and Gynecology,* vol. 187, no. 1, pp. 145-151, 2002.

[20] J. Jezewski, K. Horoba, A. Matonia, and J. Wrobel, "Quantitative analysis of contraction patterns in electrical activity signal of pregnant uterus as an alternative to mechanical approach," *Physiological Measurement,* vol. 26, no. 5, pp. 753-767, 2005.

[21] K. Horoba, J. Jezewski, J. Wrobel, and S. Graczyk, "Algorithm for detection of uterine contractions from electrohysterogram," 2001, vol. 3, pp. 2161-2164: IEEE, 2001.

[22] W. L. Maner, R. E. Garfield, H. Maul, G. Olson, and G. Saade, "Predicting term and preterm delivery with transabdominal uterine electromyography," *Obstetrics & Gynecology,* vol. 101, no. 6, pp. 1254-1260, 2003.

[23] M. Lucovnik, Z. Novak-Antolic, and R. E. Garfield, "Use of non-invasive uterine electromyography in the diagnosis of preterm labour," *Facts, Views & Vision in ObGyn,* vol. 4, no. 1, p. 66, 2012.

[24] H. Maul, W. L. Maner, G. Olson, G. R. Saade, and R. E. Garfield, "Non-invasive transabdominal uterine electromyography correlates with the strength of intrauterine pressure and is predictive of labor and delivery," *Journal of Maternal-Fetal and Neonatal Medicine,* vol. 15, no. 5, pp. 297-301, 2004.

[25] G. M. D. Haran, M. M. D. Elbaz, M. D. M. D. Fejgin, and T. M. D. Biron-Shental, "A comparison of surface acquired uterine electromyography and intrauterine pressure catheter to assess uterine activity," *American Journal of Obstetrics and Gynecology,* vol. 206, no. 5, pp. 412.e1-412.e5, 2012.

[26] "Fetal Monitoring Equipment ", ed, 2015.

[27] D. M. A. Primin, D. M. M. Budnyk, P. D. I. Chaikovsky, and P. D. V. Sosnytskyy. (2014-2015). *Department of Sensory Devices, Systems and Technologies of Noncontact Diagnostics*. Available: http://incyb.kiev.ua/eng/220.html

[28] R. Fenici, D. Brisinda, and A. M. Meloni, "Clinical application of magnetocardiography," *Experts Review of Molecular Diagnostics,* vol. 5, no. 3, pp. 291-313, 2005.

[29] R. Agarwal, A. Saini, T. Alyousef, and C. A. Umscheid, "Magnetocardiography for the Diagnosis of Coronary Artery Disease—A Systematic Review and Meta-Analysis," *Annals of Noninvasive Electrocardiology,* vol. 17, no. 4, pp. 291-298, 2012.

[30] F. Kovács, C. Horváth, Á. T. Balogh, and G. Hosszú, "Fetal phonocardiography—Past and future possibilities," *Computer Methods and Programs in Biomedicine,* vol. 104, no. 1, pp. 19-25, 2011/10/01/ 2011.

[31] Indiamart. (2019). *3D Doppler Ultrasound Machine*. Available: https://www.indiamart.com/proddetail/3d-doppler-ultrasound-machine-17861736462.html

[32] K. Benti. (2018). *Phonocardiograph (PCG) machine*. Available: http://ethiobiomed.com/phonocardiograph-pcg-machine/

[33] J. Chen, K. Phua, and Y. Song, "Development of Portable Phonocardiographic Fetal Heart Rate Monitor," *Sensors & Transducers,* vol. 95, no. 8, pp. 108-127, 2008.

[34] P. Várady, L. Wildt, Z. Benyó, and A. Hein, "An advanced method in fetal phonocardiography," *Computer Methods and Programs in Biomedicine,* vol. 71, no. 3, pp. 283-296, 2003.

[35] "Celerity PICC Tip Confirmation System," 2018.

[36] J. P. Neilson, "Fetal electrocardiogram (ECG) for fetal monitoring during labour," *Cochrane Database of Systematic Reviews,* vol. 12, no. 12, p. CD000116, 2015.

[37] C. D. J. Barras and K. A. Myers, "Nitinol – Its Use in Vascular Surgery and Other Applications," *European Journal of Vascular & Endovascular Surgery,* vol. 19, no. 6, pp. 564-569, 2000.

[38] D. M. Atlaf and D. E. Ahmad, "Design of Four degrees of freedom Manipulator with hand shaped gripper using Muscle wires," *Advances in Automation and Robotics* pp. 14-18, 11/26/2018 2013.

[39] W. B. Cross, A. H. Kariotis, and F. J. Stimler, "Nitinol characterization study," 1969.

[40] J. Whitlock. (2018). *The Uterus: Function and Anatomy*. Available: https://www.verywellhealth.com/uterus-location-function-female-anatomy-3157180

[41] P. S. La Rosa, H. Eswaran, H. Preissl, and A. Nehorai, "Multiscale forward electromagnetic model of uterine contractions during pregnancy," *BMC Medical Physics,* vol. 12, no. 1, p. 4, 2012.

[42] H. N. Aguilar and B. Mitchell, "Physiological pathways and molecular mechanisms regulating uterine contractility," *Human Reproduction Update,* vol. 16, no. 6, pp. 725-744, 2010.

[43] K. M. Myers and D. Elad, "Biomechanics of the human uterus," *Wiley Interdisciplinary Reviews: Systems Biology and Medicine,* vol. 9, no. 5, p. e1388, 2017.

[44] R. N. Miftahof and H. G. Nam, "Models of the Gravid Uterus," in *Biomechanics of the Gravid Human Uterus*: Springer, 2011, pp. 15-27.

[45] B. Sharifimajd, J. Ölvander, and J. Stålhand, "Identification of the mechanical parameters for the human uterus in vivo using intrauterine pressure measurements," *International Journal for Numerical Methods in Biomedical Engineering,* vol. 33, no. 1, pp. 1-11, 2017.

[46] A. L. Cochran and Y. Gao, "A model and simulation of uterine contractions," *Mathematics and Mechanics of Solids,* vol. 20, no. 5, pp. 540-564, 2015.

[47] L. Bursztyn, O. Eytan, A. J. Jaffa, and D. Elad, "Mathematical model of excitation-contraction in a uterine smooth muscle cell," *American Journal of Physiology-Cell Physiology,* vol. 292, no. 5, pp. C1816-C1829, 2007.

[48] W.-C. Tong, C. Y. Choi, S. Karche, A. V. Holden, H. Zhang, and M. J. Taggart, "A computational model of the ionic currents, Ca2+ dynamics and action potentials underlying contraction of isolated uterine smooth muscle," *PloS one,* vol. 6, no. 4, p. e18685, 2011.

[49] A. Rao, A. R. Srinivasa, and J. N. Reddy, "Design of shape memory alloy (SMA) actuators," vol. 3, M. Holm Altenbach, Germany, P. Lucas F.M. da Silva, Portugal , and S. Andreas Öchsner, Australia, Eds.: Springer, 2015.

[50] F. Simone, A. York, and S. Seelecke, "Design and fabrication of a three-finger prosthetic hand using SMA muscle wires," in *Bioinspiration, Biomimetics, and Bioreplication 2015*, 2015, vol. 9429, p. 94290T: International Society for Optics and Photonics.

[51] L. L. Stepan, D. S. Levi, and G. P. Carman, "A thin film nitinol heart valve," *Journal of Biomechanical Engineering,* vol. 127, no. 6, pp. 915-918, 2005.

[52] E. Kaplanoglu, "Design of shape memory alloy-based and tendon-driven actuated fingers towards a hybrid anthropomorphic prosthetic hand," *International Journal of Advanced Robotic Systems,* vol. 9, no. 3, p. 77, 2012.

[53] I. Dynalloy, "Technical Characteristics of Flexinol actuator wires," 2018, Accessed on: 1/02/2018.

[54] D. Roylance, "Pressure vessels," 2001.

[55] N. Weil, "Tensile instability of thin-walled cylinders of finite length," *International Journal of Mechanical Sciences,* vol. 5, no. 6, pp. 487-506, 1963.

[56] S. Cox, B. Hoffman, C. Werner, and F. Cunningham, *Williams Obstetrics 22nd Edition Study Guide*. McGraw-Hill Professional, 2005.

[57] K. M. Verdurmen *et al.*, "A systematic review of prenatal screening for congenital heart disease by fetal electrocardiography," *International Journal of Gynecology & Obstetrics,* vol. 135, no. 2, pp. 129-134, 2016.

[58] H.-M. Yeh *et al.*, "A new method to derive fetal heart rate from maternal abdominal electrocardiogram: monitoring fetal heart rate during cesarean section," *PloS one,* vol. 10, no. 2, p. e0117509, 2015.

[59] U. S. D. o. H. H. Services. How the Heart Works [Online]. Available: https://www.nhlbi.nih.gov/health-topics/how-heart-works

[60] J. H. van Weerd and V. M. Christoffels, "The formation and function of the cardiac conduction system," *Development*, vol. 143, no. 2, pp. 197-210, 2016.

[61] A. M. (2015, November 27th). *The Heart* Available: http://heartsite.com/html/the_heart.html

[62] D. Westbury, "Electrical activity of the heart," *British Medical Journal*, vol. 4, no. 5790, p. 799, 1971.

[63] T. W. Rooke and H. V. Sparks Jr, "The electrical activity of the heart," *Medical Physiology*, pp. 219-222, 2003.

[64] H. Staff. (2017, November 27). *Electrical System of the Heart*. Available: https://myhealth.alberta.ca/Health/Pages/conditions.aspx?hwid=te7147abc

[65] L. A. Rhodes, "The heart and its electrical system, Larry Rhodes.pdf," *Adult Congenital Heart Association* p. 2, 2008.

[66] M. Riemenschneider. (2018, November 27th). *Electrocardiogram (ECG) - Electrocardiography*. Available: https://www.cardiosecur.com/en/magazine/specialist-articles-on-the-heart/electrocardiogram-ecg/

[67] E. A. Ashley and J. Niebauer, *Cardiology explained*. Remedica, 2004.

[68] E. Karvounis, C. Papaloukas, D. Fotiadis, and L. Michalis, "Fetal heart rate extraction from composite maternal ECG using complex continuous wavelet transform," in *Computers in Cardiology, 2004*, 2004, pp. 737-740: IEEE.

[69] R. Sameni and G. D. Clifford, "A review of fetal ECG signal processing; issues and promising directions," *The Open Pacing, Electrophysiology & Therapy Journal*, vol. 3, p. 4, 2010.

Appendix A

Table A1

Detailed advantages, disadvantages, and limitations of the devices used to measure fetal heart rate and uterine contraction

Devices	Advantages	Disadvantages	Limitation
Standard TOCO-	• Non-invasive • Provides accurate info on the contraction frequency	• Information is not highly reliable for duration and intensity. • The belt use to hold the transducer (if too tight or slack will affect the quality of the trace • Not disposable	• Poor correlation with IUPC • Depends on proper placement on abdomen • Interference from maternal movement
Pneumatic TOCO–	• Lighter • Disposable • Interchangeable with standard TOCO	• There is still a need for a belt to hold the transducer in place	Not available
IUPC	• Gives quantifiable information on baseline tone, duration, amplitude and contraction.	• Invasive: need to be inserted in the uterine cavity by rupturing membrane • Increases the incidence of infection.	• Only used during labor
EHG	• Laplacian potential recording improves the spatial resolution on surface of bio-recording	• Bi and mono polar EHG recordings capture interference from other physiological signals; including abdominal muscle electrical activity, ECG, respiratory movement,.	• Reliability in detection of labor, particularly preterm labor • Bipolar and monopolar also have low spatial resolution signals recordings
CTG-	• Less instances of seizures in newborns when CTG is used	• High sensitivity to different of noise generated by material movement. • Requires frequent repositioning of transducer.	• Accuracy • False positives • Difficulty to get accurate data • Uncomfortable

Table A 1 Continued

Devices	Advantages	Disadvantages	Limitation
MCG -	• Non-invasive • Risk-free • Spatially and temporally accurate • Contactless • Fast •	• Expensive • Sensitive to metal objects and pacemakers	• Not portable • No bedside availability
MMG	• Non- invasive • Risk-free • Independent of tissue conductivity • Independent of reference	• Expensive • Sensitive to metals	• Not portable
Fetal ECG	• Non-invasive • Inexpensive method • Easy to perform • Widely available	• Restricts body movement from all of the wires and probes • Provides static picture that does not reflect severe underlying heart issues	• False negatives • Not all heart problems will show up on ECG • False positives
Doppler Ultra-sound	• Non-invasive • Helps diagnose disease	• Effected by movement of intra-abdominal structure, such as maternal vessels and fetal extremities • Prone to signal loss	• Resulting signals require signal modulation and autocorrelation to provide good quality recordings
Fetal PCG	• Cheaper than other methods ($1 vibration sensors) • Non-invasive	• Difficulty in extracting information from noisy transducer due to acoustic damping, mainly by amniotic fluid and digestive activity • Susceptibility to noise and outside sounds	• sources of sound such as the maternal breathing, fetal and maternal heart contraction, fetal movement, and shear noise due to transducer movement

Table A 2

Signal processing methods for fECG[69]

	Method	Perform ance	Computational cost	Implantation complexity	Application
Single channel	FIR/IR filtering	Low	Low	Simple	Simple frequency domain denoising
	Weiner filtering	Medium	Medium	Medium	Denoising using morphologic or spectral priors
	Wavelet denoising	Medium	Medium	Medium	More robust denoising for signal-noise mixtures with different scales
	Adaptive filtering	Medium	Medium	Medium	Low quality maternal ECG cancellation or fetal ECG enhancement for fetal HRV analysis
	Nonlinear filtering	Medium	High	Complex	Maternal ECG cancellation or fetal ECG enhancement in single and multi-channel recordings
	Kalman Filtering	High	Medium	Complex	ECG denoising, maternal ECG removal or fetal ECG enhancement having the R-peaks of the signal
Multi-channel	PCA/SV D/Factor analysis	Low	Low	simple	Dimension reduction for high-dimensional data and noise removal
	ICA	Medium	Medium/High	Medium/ complex	Blind or semi-blind decomposition of multichannel maternal-fetal mixtures

Table A 2 continued

	Method	Performance	Computational cost	Implantation complexity	Application
	πCA	Medium	Low	Simple	Decomposition of multichannel ECG mixtures having the R-peaks of the signal
	Subspace decomposition by deflation	High	Medium/high	Complex	Decomposition of (possibly) degenerate multichannel mixtures